Check for updates

Applications of Nonviral Biomaterials for microRNA Transfection in Bone Tissue Engineering

Mengyao Zhu[†], Yingzhi Gu[†], Ce Bian, Xianju Xie, Yuxing Bai and Ning Zhang*

Department of Orthodontics, School of Stomatology, Capital Medical University, Beijing, China

Bone tissue engineering, which involves scaffolds, growth factors, and cells, has been of great interest to treat bone defects in recent years. MicroRNAs (miRNAs or miRs) are small, single-stranded, noncoding RNAs that closely monitor and regulate the signaling pathway of osteoblast differentiation. Thus, the role of miRNAs in bone tissue engineering has attracted much attention. However, there are some problems when miRNAs are directly applied in the human body, including negative charge rejection of the cell membrane, nuclease degradation, immunotoxicity, and neurotoxicity. Therefore, it is necessary to use a suitable carrier to transfect miRNAs into cells. In contrast to viral vectors, nonviral vectors are advantageous because they are less immunogenic and toxic; they can deliver miRNAs with a higher molecular weight; and they are easier to construct and modify. This article reviews the application of different miRNAs or anti-miRNAs in bone tissue engineering and the related signaling pathways when they promote osteogenic gene expression and osteogenic differentiation of target cells. An overview of the properties of different types of nonviral miRNA-transfected biomaterials, including calcium phosphates, nanosystems, liposomes, nucleic acids, silk-based biomaterials, cell-penetrating peptides, bioactive glass, PEI, and exosomes, is also provided. In addition, the evaluations in load efficiency, release efficiency, cell uptake rate, biocompatibility, stability, and biological immunity of nonviral miRNA-transfected biomaterials are given. This article also confirms that these biomaterials stably deliver miRNA to promote osteogenic gene expression, osteogenic differentiation of target cells, and mineralization of the extracellular matrix. Because there are differences in the properties of various nonviral materials, future work will focus on identifying suitable transfection materials and improving the transfection efficiency and biocompatibility of materials.

Keywords: bone tissue engineering, microRNA, calcium phosphates, nanoparticles, transfection, nonviral vectors, osteogenesis

1 INTRODUCTION

1.1 Bone Tissue Engineering

Bone defects caused by disease, trauma, or surgery are common clinical problems encountered by plastic surgeons. Severe bone defects can result in delayed bone union, leading to a high disability rate. The self-healing ability of bone defects is strong, but the self-healing of large-scale bone defects is often delayed or impossible, thereby requiring external intervention. Traditional bone defect repair methods include autogenous and allogeneic bone transplantation, but these methods have

FIGURE 1 | The procession of the microRNA-involved bone tissue engineering. **(A)** Nonviral vectors and microRNA are combined *in vitro*. **(B)** Stem cells are cultured, expanded, and transfected *in vitro*. **(C)** The cells are then seeded onto a scaffold material. **(D)** The scaffold with cells is transplanted to the corresponding defect site of the animal model. **(E)** Cells continue to grow and reproduce *in vivo* and secrete extracellular matrix. With the gradual degradation of the materials, the new bone tissue finally replaces the scaffold materials to repair the structure and restore the function.

limitations. Although the former is the "gold standard" of bone transplantation, it has the disadvantages of limited materials, complications at the donor site, and the need for secondary surgery. Furthermore, the latter may lead to disease transmission, injection reactions, and poor prognosis due to its reduced osteoinduction capacity (Wang and Yeung, 2017; Han et al., 2020). Therefore, bone tissue engineering has emerged and has been developed in the past 2 decades. Bone tissue engineering involves culturing and expanding stem cells *in vitro*. The cells are then seeded onto a scaffold material with good biological activity and degradability, and the cells are cultivated for a period of time. Later, the scaffold with cells is transplanted to the corresponding defect site. Cells continue to grow and reproduce *in vivo* and secrete extracellular matrix. With the gradual degradation of the materials, the new bone tissue finally replaces the scaffold materials to repair the structure and restore the function (Qu et al., 2019). (**Figure 1**) As an alternative to bone defect repair, bone tissue engineering reduces the defects of autologous bone transplantation and allogeneic bone transplantation. The goal of bone tissue engineering is to employ the biochemical signaling pathway during the natural bone healing process to promote self-healing and bone regeneration to restore and maintain bone morphology and function (Arriaga et al., 2019). This technology involves the use of scaffold biomaterials and the introduction of appropriate growth factors and multipotent cells (Marew and Birhanu, 2021). Currently, through bone tissue engineering technology, many new bioactive materials and technologies have been developed, such as three-dimensional (3D)-printed scaffolds (Zhang et al., 2019) and gene delivery technology (Gantenbein et al., 2020), to reduce the shortcomings of traditional transplantation methods and improve the biocompatibility and the osteogenic,

osteoconductive, and osteoinductive properties of grafts. The study of the molecular mechanism of osteogenesis induced by these biomaterials is also a hot field.

1.2 miRNAs in Bone Tissue Engineering
1.2.1 Mechanism of miRNAs in Bone Tissue Engineering

Bioactive factors used in bone tissue engineering include the following three categories: 1) growth factors, 2) genetic substances, and 3) drugs (Dasari et al., 2022). The main effect of drug delivery is to resist local inflammation, to reduce the immune response, and to provide bone nutrition in bone tissue engineering. Drug delivery has a small effect on promoting osteogenesis. Growth factors have been widely used in bone tissue engineering; they bind to cell surface receptors to induce cell migration, differentiation, and proliferation, among which bone morphogenic protein (BMP) is the most commonly used (Fuerkaiti et al., 2022). However, the cost of synthesizing enough growth factors for clinical use is high, and proteolytic degradation easily occurs, resulting in a short half-life of the biological activity. Thus, the delivery of genetic material, which includes DNA and RNA, is a good alternative to growth factor delivery (Samorezov and Alsberg, 2015). This review mainly discusses the delivery of microRNAs (miRNAs or miRs).

miRNAs are small, single-stranded, noncoding RNAs that mainly exist in cells, and a small amount exist in extracellular environments, such as serum, plasma, and tears (Lanzillotti et al., 2021). MiRNAs are a class of regulators of gene expression (Reda El Sayed et al., 2021). By affecting the translation of target messenger RNAs (mRNAs), miRNAs can negatively regulate gene expression at the posttranscriptional level. miRNAs are able to bind the 3′ untranslated region (3′-UTR) of target mRNAs, which are subsequently degraded or translationally
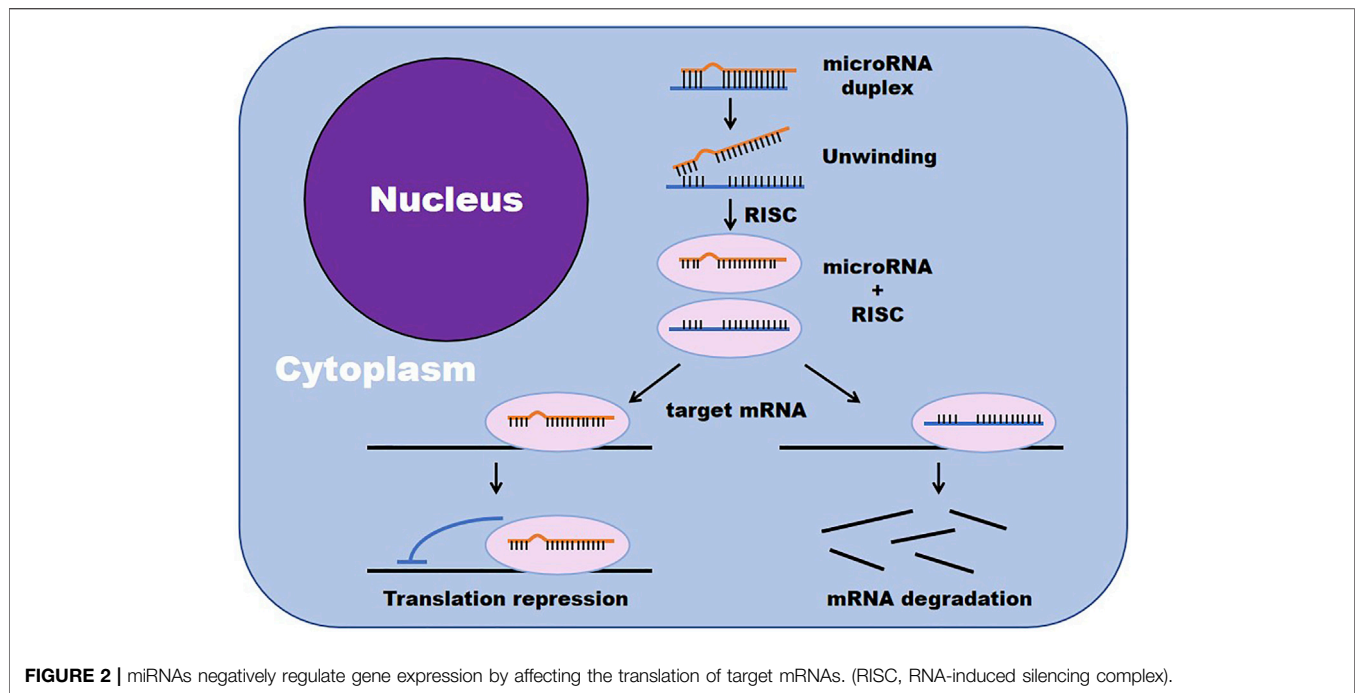
FIGURE 2 | miRNAs negatively regulate gene expression by affecting the translation of target mRNAs. (RISC, RNA-induced silencing complex).

silenced, to regulate cell proliferation, differentiation and apoptosis (**Figure 2**) (Mazziotta et al., 2021).

miRNAs play an important role in bone formation involving mesenchymal stem cells (MSCs) derived from blood, pericytes, and bone marrow (Iaquinta et al., 2019; Liu J. et al., 2019). miRNAs promote or inhibit osteogenic differentiation by targeting transcription factor gene expression or targeting either positive or negative regulatory genes associated with osteogenesis (Lanzillotti et al., 2021). During the process of MSC differentiation into osteoblasts, miRNAs closely monitor and regulate the following two key signaling cascades: the transforming growth factor-beta (TGF-β)/BMP pathway and the Wingless/Int-1(Wnt)/β-catenin signaling pathway (Mazziotta et al., 2021). For example, miR-93-5p suppresses osteogenic differentiation in a rabbit model of traumatic femoral head necrosis by binding the 3′-UTR of Smad5 and reducing BMP-2 and RUNX2 (Zhang Y. et al., 2021). Xu et al. confirmed that miR-889 binds the 3′UTR of WNT7A and negatively regulates the osteogenic differentiation of bone mesenchymal stem cells (BMSCs) through the Wnt/β-catenin signaling pathway (Xu et al., 2019). In addition, miR-486-3p activates the Wnt/β-catenin signaling pathway by targeting catenin beta interacting protein 1 (CTNNBIP1) to promote the osteogenesis of BMSCs, which has been confirmed in bone marrow samples from patients with osteoporosis and in mice undergoing ovariectomy (Zhang Z. et al., 2021). In addition, in other cells, such as fibroblasts, miRNAs regulate osteogenesis through similar signaling pathways. Ding et al. obtained fibroblasts from the capsular ligament of patients with ankylosing spondylitis and studied its osteogenic differentiation mechanism, and they reported that miR-214-3p targets the BMP2 gene and blocks the BMP-TGFβ axis, thereby

preventing fibroblast osteogenesis (Ding et al., 2020). Apart from these two pathways, some miRNAs regulate bone differentiation through other signaling pathways, such as the Notch signaling pathway and Nrf2 pathway (Wang et al., 2013; Liu H. et al., 2019). In conclusion, the miRNAs that have been applied to bone tissue engineering and tested *in vivo* are listed in **Table 1**, and their known mechanisms of regulating osteogenic differentiation are listed in **Table 2**.

1.2.2 Evaluation of Osteogenic Effect of miRNA

The existing *in vivo* and *in vitro* studies have confirmed that miRNA can effectively promote bone regeneration. The main observation indexes of *in vitro* experiments are target mRNA and protein, Runx2, ALP, and the osteoblast-specific microRNA (Raj Preeth et al., 2021). The main indexes of *in vivo* experiments are as follows: significant improvement of bone volume fraction (bone volume/total volume, BV/TV), thickness of trabecularized spicules (Tb.Th), and trabecular number (Tb.N) (Kureel et al., 2017), bone mineral density (BMD) (Wu et al., 2018), bone mineral content (BMC) (Yang et al., 2019), bone surface density (bone surface/bone volume, BS/BV) (Gan et al., 2021), trabecular spacing (Tb.Sp), trabecular bone pattern factor (TbPF) (Zhou et al., 2021), and higher percentage of bone area to total area (BA/TA) (Liu H. et al., 2019).

1.3 Biomaterials for miRNA Transfection in Bone Tissue Engineering

Based on the understanding of the RNA expression profile in tissues and diseases, miRNA delivery strategies have been

TABLE 1 | The application of miRNAs in bone tissue engineering *in vivo*.

miRNA	Other bioactive factor	Transfection agent	Biomaterial scaffold	Cell type	Animal model	Timepoint	Results	References
miR let-7d		Layered double hydroxide (LDH) nanoparticles	Fibrin Gel	BMSCs	subcutaneous pockets on the backs of the athymic nude mice (Subcutaneous Ectopic Osteogenesis Model)	2 weeks	Significant improvement of bone volume fraction (bone volume/total volume, BV/TV)	Yang L et al. (2021)
miR-10a	IL-2, TGF-β	PLLA/PEG co-functionalized MSN, PLGA MS	PLLA nanofibrous spongy microspheres (NF-SMS)	--	Mouse periodontal disease model	10 days	Substantially rescue the alveolar bone loss	Liu et al. (2018b)
antimiR-138	SDF-1α	Chitosan/tripolyphosphate/hyaluronic acid/antimiRNA-138 nanoparticles (CTH/antimiR-138 NPs)	Thermosensitive chitosan/β-glycerol phosphate (CS/GP) hydrogel	--	8 mm calvarial defect in rats	8 weeks	Higher regenerated bone (32.74 ± 4.89%), higher BMD of newly formed bone, greater Tb.N (0.90 ± 0.05)	Wu et al. (2018)
miR-19b-3p		Lentivirus	PLLA/POSS	BMSCs	8 mm calvarial defect in rats	3 months	Almost complete repair of bone defects and higher bone mineral density	Xiong et al. (2020)
miR-20a		Poly(ethylene glycol) (PEG) hydrogels		hMSCs	5 mm calvarial defect in rats	12 weeks	Significantly higher average bone volume fraction (24.51%), significantly higher trabecular number and lower trabecular separation	Nguyen et al. (2018)
miR-21		Nanocapsules	O-carboxymethyl chitosan (CMCS)	--	2 mm diameter bilateral bone defects of the proximal tibia in rats with bilateral ovaries removal	4 weeks	At 4 weeks: significantly higher BV/TV and Tb.Th, higher calcium nodule formation; at 8 weeks: less new cancellous bone, lower BV/TV, lower Tb.Th, the new cancellous bone had been absorbed and the marrow cavity had been dredged	Sun et al. (2020)
miR-21		Nanocapsules and O-carboxymethyl chitosan (CMCS) powder mixed gel	Titanium cylinders	--	New Zealand White rabbits	3 months	Increased content of mineral (Ca and P), plenty of nodules, a dense structure combined with collagenous fiber and apatite, similar to mature bone	Geng et al. (2020)
miR-21		Lentivirus	β-TCP	rBMSCs	5 mm calvarial defect in rats	60 days	higher BMD and Tb.Th	Yang et al. (2019)
		Lentivirus	β-TCP	BMSCs	20 mm × 10 mm osteoperiosteal segmental defect in canine mandibular	6 months	Higher BV/TV, BMD, bone mineral content (BMC), improved percentage of new bone area (52.21 ± 3.87%), lower percentage of the β-TCP residual area (6.82 ± 1.43%)	

TABLE 1 | (*Continued*) The application of miRNAs in bone tissue engineering *in vivo*.

miRNA	Other bioactive factor	Transfection agent	Biomaterial scaffold	Cell type	Animal model	Timepoint	Results	References
miR-21		N-(3-aminopropyl) methacrylamide, acrylamide, and ethylene glycol dimethacrylate nanocapsules	Titanium (Ti)-based SrHA/miR-21 composite coating	Osteoblast-like MG63 cells	4 mm defect at distal femur and tibia in New Zealand white rabbits	3 months	Significantly higher bone-implant contact, higher biomechanical strength (287 ± 25 N), highest $v1PO43-/$ amide I values (13.1 ± 1.4)	Geng et al. (2018)
miR-21		Nanocapsules	O-carboxymethyl chitosan (CMCS) network		3 mm tibial plateau bone defect in rats	8 weeks	Significantly higher BV/TV, 2.4-fold bone formation	Meng et al. (2016b)
miR-26a		Injectable poly(ethylene glycol) (PEG) hydrogel	--	hMSCs	7 mm calvarial defect in rats	8 weeks	Statistically increase in BV/TV and bone surface density (bone surface/bone volume, BS/BV)	Gan et al. (2021)
miR-26a		A comb-shaped polycation (HA-SS-PGEA) consisting of hyaluronic acid (HA), disulfide groups, and ethanolamine (EA)-functionalized poly(glycidyl methacrylate) (PGMA)	Three-dimensional (3D) hybrid nanofiber aerogels	BMSCs	8 mm diameter cranial defect in rats	4 weeks	Much larger defect healing area (new bone volumes: 21.8 mm^3, corresponding closure percentages: 62.2%, coverage: 56.4%)	Li et al. (2020)
antimiR-26a-5p		Lentivirus	Biphasic calcium phosphate (BCP)	Adipose-derived mesenchymal stem cells (ADSCs)	4 mm-long ×2 mm-deep femoral defect in rats	2\4\8 weeks	Significantly higher BV/TV (8 weeks), higher BMD (2, 4 weeks), higher Tb.N. (2, 4 weeks), higher Tb.Th (2, 4 weeks), lower residual bcp/TV	Yuan et al. (2019)
miR-26a		lentivirus	β-TCP	mBMSCs	5 mm calvarial defect in mice	2 months	A marked increase in the volume of newly formed bones, which almost filled the whole defect area	Liu et al. (2018a)
miR-26a		siPORT NeoFX transfection agent	HyStem-HP™ hydrogel	mBMMSCs	ectopic bone formation model of immunocompromised mice	8 weeks	significantly more bone formation and high density of blood vessels	Li et al. (2013)
		siPORT NeoFX transfection agent	HyStem-HP™ hydrogel	mBMMSCs	5 mm calvarial defect in mice	12 weeks	increasing vascular volume showed by immunofluorescence staining for CD31	
miR-29b-3p	pTRE2-Tet-on plasmid	microbubble-ultrasound system	--	--	femoral fracture in mice	6 weeks	significant reduction in callus area, higher BV/TV (including BVh/TV, BVl/TV, BV$_1$/TV) and BMD, enhanced stiffness and relative stiffness	Lee et al. (2016)
miR-29b		O-carboxymethyl chitosan (CMCS) coating nanocapsules	titanium Alloy	--	3 mm tibial defect in rats	8 weeks	significantly higher rate of calcification (2.80-fold), 24% increase in BIC, more new bone (~2.01-fold at 2 weeks)	Meng et al. (2016a)

(Continued on following page)

TABLE 1 | (*Continued*) The application of miRNAs in bone tissue engineering *in vivo*.

miRNA	Other bioactive factor	Transfection agent	Biomaterial scaffold	Cell type	Animal model	Timepoint	Results	References
as-miR-31		lentivirus	β-tricalcium phosphate (β-TCP)	rat ASCs	5 mm calvarial defect in rats	8 weeks	higher BMD (0.553 ± 0.081 g/cm3), BV/TV (35.42 ± 6.12%), new bone formation at 2 weeks: 4.58 ± 0.51%, 4 weeks: 7.62 ± 1.18%, 6 weeks: 8.11 ± 0.89%, 8 weeks: 36.81 ± 3.54%)	Deng et al. (2013)
antimiR-31		lentivirus	poly (glycerol sebacate) (PGS)	rat BMSCs	8 mm calvarial defect in rats	8 weeks	higher BV/TV (41.82 ± 6.54%), BMD (0.492 ± 0.062 g/cm^3), and percentage of new bone area (60.92 ± 7.34%)	Deng et al. (2014)
miR-33a-5p		Lipofectamine 3000	collagen-based hydrogels	hASCs	ectopic bone formation model of nude mice	8 weeks	more newly constructed bone, more collagen fiber bundles arranged compactly	Shen et al. (2020)
miR-34a		Lipofectamine 2000		rBMSCs	ectopic bone formation model of nude mice	8 weeks	significantly higher percentage of bone area to total area (BA/TA)	Liu J et al. (2019)
		Lipofectamine 2000	collagen-based hydrogel	--	3 mm tibial defect in rats	8 weeks	significantly higher BV/TV	
miR-92b		lentivirus		MSC	ectopic bone formation model of nude mice	8 weeks	miR-92b was superior to GFP in ectopic bone formation by HE staining	Hou et al. (2021)
					open femur fracture model of rats	3 weeks	higher newly formed bone, higher volume of low-density bone/total tissue volume, higher percentage of bone in callus	
miR-93-5p inhibitor		Lipofectamine 2000	--	rabbit BMSCs	Trauma-induced osteonecrosis of the femoral head (TIONFH) rabbit model	8 weeks	significantly fewer empty lacunae and more osteoblasts	Zhang Y et al. (2021)
miR-106a Inhibitor		Liposome 2000	autologous oxygen release nano-bionic scaffold	rBMSCs	rat tibia fracture model	6 weeks	markedly higher BMD, significantly promoted collagen II production	Sun et al. (2018)
miR-129-5p		lentivirus	matrigel	BMSCs	3 mm diameter defect on each side of the calvaria in mice	8 weeks	much higher BV/TV (0.702 ± 0.027), significantly higher BMD (1,296 ± 53 g/cm3), more bone-like structures and collagen deposits	Zhao et al. (2021)
miR-133a		aspartate, serine, serine (AspSerSer) 6-liposome	--	osteoblast	hindlimb unloading (HU)-challenged mice	3 weeks	less bone loss and osteoclast numbers, enhanced BMD, BV/TV, Tb.Th and Tb.N, lower Tb.Sp, trabecular bone pattern factor (TbPF) and BS/BV	Zhou et al. (2021)

TABLE 1 | (*Continued*) The application of miRNAs in bone tissue engineering *in vivo*.

miRNA	Other bioactive factor	Transfection agent	Biomaterial scaffold	Cell type	Animal model	Timepoint	Results	References
antagomiR-133a		collagen-hydroxyapatite (coll-HA)	coll-nHA	--	7 mm calvarial defect in rats	4 weeks	statistically more calcified tissue (8.71 ± 7.48%), statistically more and thicker new trabeculae, statistically more *de novo* bone (≥70% increase)	Castaño et al. (2020)
antagomiR-133a/b		CTH nanoparticle (chitosan solution (CS), Sodium tripolyphosphate (TPP), hyaluronic acid (HA))	--		5 mm calvarial defect in mice	12 weeks	significantly increased new bone area	Jiang et al. (2020)
miR-135		lentivirus	PSeD	rat ADSCs	8 mm calvarial defect in rats	8 weeks	significantly higher BV/TV (50.53 ± 4.45%), BMD (0.0165 ± 0.0012 g/cc) and Tb.N (0.3352 ± 0.0529), larger newly formed bone (820.4 ± 77.3 mm^2), higher percentage of newly formed bone in the total area of bone tissue (40.13 ± 1.94%), larger area of fluorochrome stained bone	Xie et al. (2016)
miR-142-5p		periosteal injection at the fracture site	--	--	femoral fracture in mice	4 weeks	significantly higher BMD	Tu et al. (2017)
miR-146a inhibitor		lentivirus	poly (sebacoyl diglyceride) (PSeD) porous scaffold	rat ADSCs	8 mm calvarial defect in rats	8 weeks	significantly higher BV/TV, Tb.N and BMD (49.8 ± 5.49%, 0.4094 ± 0.0687, 0.01581 ± 0.00299 g/cc), larger new bone areas in weeks 2–4: 92.38 ± 16.69 mm^2, weeks 4–6: 115.32 ± 11.87 mm^2, and weeks 6–8: 90.93 ± 9.95 mm^2	Xie et al. (2017)
miR-148a-3p		lentiviruses	--	BMSCs	ovariectomy (OVX)-induced osteoporosis model in mice	6 weeks	higher BMD, BV/TV ratio, Tb.N and Tb.Th, lower trabecular spacing (Tb.Sp)	Liu and Sun, (2021)
miR-148b		(hydroxypropyl) cellulose (HPC)-modified silver nanoparticles (SNPs)	collagen-infilled 3D printed hybrid	rBMSCs	5 mm in diameter and 1 mm in thickness calvarial defect in rats	8 weeks	significantly higher BV/TV (%), higher normalized BMD (34.7 ± 8.9%), larger bone coverage area (78.1 ± 20.8%), higher connectivity density (2.86 ± 1.23)	Moncal et al. (2019)

(Continued on following page)

TABLE 1 | (*Continued*) The application of miRNAs in bone tissue engineering *in vivo*.

miRNA	Other bioactive factor	Transfection agent	Biomaterial scaffold	Cell type	Animal model	Timepoint	Results	References
miR-148b	BMP-2	baculovirus	poly (L-*lactide*-co-*glycolide*) (PLGA)	hASCs	4 mm calvarial defect in nude mice	12 weeks	the new bone nearly filled the entire defect after 12W, higher bone area (94.7 ± 0.8%), volume (89.4 ± 11.1%) and density (95.7 ± 3.9%)	Liao et al. (2014)
miR-187		lentivirus		hMSCs	osteoporosis (OP) mouse model	28 days	significantly reverse the decreased bone healing rate	Zhang J et al. (2021)
agomiR-199a-5p		chitosan nanoparticles	hydroxyapatite/collagen (HA/collagen)	hMSC	ectopic bone formation model of NOD/SCID mice	6 weeks	higher density, darker MSCs and more collagen deposition in Masson trichrome staining for collagen higher density, more regenerated bone in the center of the repaired area	Chen X et al. (2015)
		chitosan nanoparticles	fibrin gel	--	3 mm tibial defect in rats	8 weeks		
miR-200c		pDNA	3D-printed β-tricalcium phosphate (β-TCP) with collagen coatings	BMSCs	9 mm diameter parietal defect in rats	4 weeks	statistically increase in bone formation	Remy et al. (2021)
miR-205		lentivirus		endothelial colony-forming cells (ECFCs)	mandibular distraction osteogenesis (MDO) canine model	4 weeks	the distraction gap was fully bridged	Jiang et al. (2021)
miR-210	simvastatin (Siv)	dual-sized pore structure calcium-silicon nanospheres (DPNPs)	β-TCP	--	5 mm calvarial defect in mice	8 weeks	the highest bone density and bone volume, strong positive expression of CD31 (the platelet endothelial cell adhesion molecule-1)	Liu et al. (2021)
miR-222	aspirin	mesoporous silica nanoparticles (MSN)	injectable colloidal hydrogel	--	5 mm mandibular defect in rats	10 weeks	higher BV/TV% (21.97% ± 3.99%), significant increased neurogenic proteins expression	Lei et al. (2019)
antimiR-222		Lipofectamine 2000	HA/tricalcium phosphate (HA/TCP)	hBMSCs	ectopic bone formation model of non-obese diabetic/severe combined immunodeficiency (NOD/SCID) mice	8 weeks	statistically higher quantified bone volume (% bone/total area)	Chang et al. (2018)
miR-335-5p		lipidoid nanoparticles	empty silk scaffold (SS)	mBMSCs	4 mm calvarial defect in mice	5 weeks	significantly higher BV/TV	Sui et al. (2018)
miR-335-5p		tetrahedral DNA nanostructures (TDNs)	Heparin lithium hydrogel (Li-hep-gel)	BMSCs	3 mm femoral defect in rabbits	12 weeks	70% new bone area, new blood vessels 12n, empty lacunae 22% ± 6%	Li et al. (2022)
antimiR-467g		Lipofectamine RNAi MAX	--	mouse calvarial osteoblast (MCO) cells	0.8 mm femoral defect in mice	21 days	significantly higher BV/TV, Tb.Th and Tb.N	Kureel et al. (2017)

(Continued on following page)

TABLE 1 | (*Continued*) The application of miRNAs in bone tissue engineering *in vivo*.

miRNA	Other bioactive factor	Transfection agent	Biomaterial scaffold	Cell type	Animal model	Timepoint	Results	References
miR-672		lentivirus	CPC	ADSCs	5 mm critical size skull defect in rats	8 weeks	highest blood vessel volume and number (3.56 ± 6.46 mm^3, 15.43 ± 7.67 mm^{-2}), enhanced BMD(0.78 g ± 4.28cm^{-3}), BV/TV (17.83 ± 8.42%), significantly higher new bone area and new bone area/total area	Chen et al. (2021)
miR-2861		sticky-end tetrahedral framework nucleic acids (stFNAs)		BMSCs	1 mm spherical femoral defect in mice	2 weeks	The surface defect had almost completely healed after 2 weeks	Li X et al. (2021)
miR-5106		novel monodispersed bioactive glass nanoclusters (BGNCs) with PEI	hydrogel	BMSCs	5 mm calvarial defect in rats	4 weeks	significantly high new bone volume and trabecular thickness	Xue et al. (2017)

developed to enhance osteogenesis, such as using miRNA replacement therapy to administer double-stranded oligonucleotide miRNA mimics to treat conditions in which the target genes are overexpressed due to miRNA downregulation (Sriram et al., 2015). However, there are some difficulties when RNAs are directly applied in the human body. First, miRNA is a negatively charged molecule, which itself has difficulty penetrating the negatively charged cell membrane (Samorezov and Alsberg, 2015). Second, unmodified miRNA antagonists and miRNA mimics are rapidly degraded and eliminated in the blood circulation by nucleases that are rich in the patient bloodstream (Grixti et al., 2021). Third, miRNAs can lead to immunotoxicity by activating interferons or Toll-like receptors (Md et al., 2021) and neurotoxicity by triggering neurodegeneration through Toll-like receptors (Chen Y. et al., 2015). Therefore, it is necessary to use a suitable carrier to deliver miRNAs to protect them from inactivation in the process of matrix formation, storage, and release. The carrier should also deliver miRNA to specific tissues or organs continuously, stably and efficiently as well as ensure efficient cell uptake (Meng et al., 2016b). For most miRNA therapies developed thus far, cells are transfected or transduced with miRNAs or anti-miRNAs and loaded into scaffolds that are implanted into target sites rather than locally releasing the miRNAs/anti-miRNAs directly from scaffolds. Therefore, future research may focus on developing miR carriers to deliver miRNA/anti-miRNAs to cells *in vivo* (Arriaga et al., 2019).

RNA carriers are divided into viral vectors and nonviral vectors. Viral gene delivery methods present some intrinsic drawbacks, including difficult production processes (Tarach and Janaszewska, 2021), triggering acute inflammation, delayed humeral or cellular immune reactions (Levingstone et al., 2020), foreign DNA insertional mutagenesis (Dasgupta and Chatterjee, 2021), and limitation of insert molecule size (Nayerossadat et al., 2012). In contrast, nonviral vectors are advantageous due to their following properties: They are less immunogenic and toxic, they can deliver miRNAs with a higher molecular weight, and they are easier to construct and modify (Levingstone et al., 2020). The binding modes of miRNA and transfection agents (as illustrated in **Table 3**) mainly include electrostatic interactions (Liu et al., 2018b; Yang L. et al., 2021; Hosseinpour et al., 2021), hydrogen bonding (Meng et al., 2016b; Geng et al., 2018), polymer network wrapping (Geng et al., 2018), chemical crosslinking (Moncal et al., 2019), physical adsorption (Yu et al., 2017), and photosensitive linking (Qureshi et al., 2013; Gan et al., 2021). In addition, nonviral vectors can also transport synthetic siRNA and miRNA mimics, thus avoiding the need for nuclear localization performed according to plasmid DNA (pDNA) constructs containing RNA interference (RNAi) expression cassettes (Gantenbein et al., 2020). This effect allows siRNA/miRNA mimics to interact with the RNAi machinery directly in the cytosol, reducing the degree of intracellular trafficking required for RNAi-mediated gene repression and silencing (Levingstone et al., 2020).

To our knowledge, this article is the first review to summary and compare the characteristics of different types of nonviral miRNA-loaded biomaterials to provide examples of their application in *in vitro* or *in vivo* experiments in the future. In addition, the review confirms that nonviral miRNA vector materials can stably transmit miRNA. We also discuss the application prospects of miRNAs in bone tissue engineering.

TABLE 2 | The mechanism of miRNAs tested *in vivo* regulating osteogenic differentiation.

miRNAs	Pathway	Related signaling pathways	Cell types	References
miR-1-3p	SOX9 pathway	miR-1-3p targets and decreases Sox9 transcription factor activity. Sox9 negatively regulates Runx2 and type X collagen expression to modulate endochondral ossification-related disorders. Ding et al. (2021)	BMSCs	Ding et al. (2021)
miR-10a	TGF-β pathway	Interleukin 2 (IL-2) and transforming growth factor beta (TGF-β) are cytokines known to enhance Treg recruitment, proliferation, and differentiation. miR-10a can facilitate naïve T cells to differentiate to Tregs. The higher number and possibly more mature Tregs substantially suppressed the destructive osteoclastogenesis and enhanced the osteoblastic activity, synergistically rescuing periodontal bone loss	mice T cells	Liu et al. (2018b)
miR-let-7d	BMP pathway	miRNA-let-7d targets the 3′-UTR of HMGA2, resulting in the suppression of the expression of GSK3β protein, positively regulating osteogenic differentiation and negatively regulates adipogenic differentiation of hADSCs	human adipose-derived mesenchymal stem cells (hADSCs) BMSCs	Wei et al. (2014) Yang L et al. (2021)
miR-19b-3p	BMP pathway	miR-19b-3p could bind to the 3′UTR of Smurf1, suppressing the expression of Smurf1 which is a negative regulator of osteogenesis. Smurf1 could mediate Runx2 degradation to inhibit osteoblast differentiation and bone formation. Smurf1 can also mediate the degradation of Smad1/5 which is the down-stream factor of BMP signal channel, resulting in the suppression of the osteoblast differentiation	BMSCs	Xiong et al. (2020)
miR-20a	BMP pathway	miRNA-20a has a positive effect on hMSC osteogenic differentiation by inhibiting the expression of PPAR-γ, a down regulator of BMP signaling in osteogenesis	hMSCs	Nguyen et al. (2018)
miR-21	PI3K-AKT signaling pathway	miR-21 directly targets and inhibits PTEN by binding its 3′-UTR, thus leading to the activation of AKT and HIF-1α. The PI3K-AKT signaling pathway activity has an increasing tendency responding to miR-21 up-regulation. This enhancement promotes the phosphorylation of GSK-3β, leading to the stabilization and high concentration accumulation of β-catenin in cytoplasm to activate the transcription of RUNX-2, and finally increases the osteogenesis of hUMSCs	hUMSCs	Meng et al. (2015); Yang et al. (2019)
miR-26a	BMP pathway	miR-26a interacts with the 3′-UTR of the Smad1 mRNA, diminishing the availability of the active SMAD1 transcription factor to participate in the differentiation process of hADSCs and elevating the mRNA and protein expression levels of Runx2. SMAD1 is the downstream effector of BMP signaling, and it is phosphorylated by BMP type I receptors	hADSCs	Gan et al. (2021); Liu et al. (2018a)
	Wnt/β-catenin pathway	miRNA-26a targets the 3′-UTR of GSK3 β to activate Wnt signaling for promoting osteogenic differentiation of BMSCs by inhibiting the expression of GSK3β and increasing the level of active β-catenin	BMSCs	Su et al. (2015)
		miR-26a-5p inhibits the translation of Wnt5a by directly binding to the 3′-UTR of Wnt5a. WNT5A is a noncanonical Wnt ligand and activates two noncanonical Wnt pathways, one of which is the Wnt/Ca2+ signaling pathway. Yuan et al. (2019)	ADSCs	Yuan et al. (2019)
miR-29b	M-CSF and RANK-L signaling pathways	miR-29b targets C-FOS and MMP2 within osteoclasts (OCLs). In OCL precursors, M-CSF promotes RANK expression through C-FOS and sustains survival and cytoskeletal reorganization. RANK controls NFKB activation, which in turn leads to upregulated expression of NFATc-1, the master transcription factor for OCL generation and function. MMP2 belongs to the gelatinase protein family and participates to bone matrix degradation	osteoclast (OCL)	Rossi et al. (2013)
miR-31	BMP pathway	miR-31 typically binds to the mRNA and targets and inhibits the translation of the master transcription factor special AT-rich sequence-binding protein 2 (Satb2). SATB2 interacts with and enhances the transcriptional activity of Runx2 and activating transcription factor 4 (ATF4) Yan et al. (2011). As-miR-31 promotes bone regeneration and bone defect repair	BMSCs	Deng et al. (2014)

(Continued on following page)

TABLE 2 | (*Continued*) The mechanism of miRNAs tested *in vivo* regulating osteogenic differentiation.

miRNAs	Pathway	Related signaling pathways	Cell types	References
miR-33a-5p	circFOXP1/miR-33a-5p/FOXP1 pathway	miR-33a-5p inhibits osteogenesis by targeting forkhead box P1 (FOXP1) 3′-UTR and down-regulating FOXP1 expression (Shen et al., 2020). FOXP1 regulates cell-fate choice of MSCs through interactions with the CEBPβ/δ complex and recombination signal binding protein for immunoglobulin κ J region (RBPjκ), key modulators of adipogenesis and osteogenesis, respectively. Li X et al. (2017)	hASCs	Li X et al. (2017); Shen et al. (2020)
miR-34a	Notch signaling pathway	miR-34a directly targets Notch1, improving the osteogenic differentiation of irradiated BMSCs by suppressing NOTCH1, since downregulation of NOTCH1 enhanced the mRNA and protein expression of RUNX2 and OCN.	BMSCs	Liu J et al. (2019)
mir-92b	ERK and JNK signaling pathways	Ezh2 is a potential target of mir-92b and down-regulated by it. Ezh2 is the catalytic subunit of the Polycomb Repressive Complex 2 (PRC2) and catalyzes tri-methylation of histone H3 at lysine 27 (H3K27me3) to silence target genes. And extracellular signal-regulated kinases (ERK) and c-Jun N-terminal protein kinase (JNK) signaling pathways were activated by mir-92b, which could finally lead to the enhanced osteogenesis of MSCs	MSCs	Hou et al. (2021)
miR-93-5p	BMP-2/Smad5 pathway	miR-93-5p suppresses osteogenic differentiation of BMSCs by binding the 3′-UTR of Smad5 and reducing BMP-2 and RUNX2	BMSCs	Zhang Y et al. (2021)
miR-106a	BMP-2/Smad5 pathway	miR-106b-5p regulates Smad5 expression negatively, and they functioned as an inhibitory factor in the physiological process of bone formation and osteoblast differentiation. Smad5 is a downstream transcription factor phosphorylated and activated by of BMP-2 receptors which is a key signaling component in osteoblast differentiation, a member of TGF-β superfamily. The phosphorylated Smad5 forms a complex with Smad4 (Co-Smad), then translocates into the nucleus to activate transcription factor Cbfa1/Runx2	BMSCs	Fang et al. (2016)
miR-129-5p	Wnt/β-catenin pathway	miR-129-5p targets the 3′-UTR of Dickkopf3 (Dkk3) and repress it to enhance osteoblast differentiation. Dkk3 could bind to β-catenin, mediating Wnt signaling pathway	BMSCs	Zhao et al. (2021)
miR-133	BMP pathway	MiR-133 directly regulates the 3′UTR of distal-less homeobox 3 (Dlx3), a member of the Dlx family of homeobox proteins. It is a transcriptional activator of runt-related transcription factor 2 (Runx2) during osteogenic differentiation. Mir-133a inhibits Dlx3 expression *via* direct targeting of the Dlx3 3′-UTR.	MSCs	Qadir et al. (2018)
		miR-133 inhibits the bone formation by targeting the 3′-UTR of RUNX2 and decreasing the expression level of RUNX2Peng et al. (2018); Jiang et al. (2020)	osteoblasts	Zhou et al. (2021)
miR-135	Hoxa2/Runx2 pathway	miR-135 negatively regulates Hoxa2 expression by targeting the 3′-UTR of Hoxa2. And Hoxa2 negatively regulates Runx2 expression in ADSCs. The overexpression of miR-135 enhances the expression of bone markers and extracellular matrix calcium deposition	ADSCs	Xie et al. (2016)
antimiR-138	ERK1/2 pathway	The antimiR-138 delivery down-regulates the endogenous miR-138 levels in BMSC sheets, activates the extracellular signal regulated kinases 1/2 (ERK1/2) pathway and enhances the expression of RUNX2 finally leading to enhanced osteogenesis	BMSCs	Yan et al. (2014)
miR-142-5p	Ubiquitination pathway	miR-142-5p promotes osteoblast activity and matrix mineralization by targeting the gene encoding WW-domain-containing E3 ubiquitin protein ligase 1. And miR-142-5p stimulates osteocalcin and Runx2 expression by targeting Wwp1. Agomir-142-5p in the fracture areas stimulates osteoblast activity	preosteoblast cells	Tu et al. (2017)
miR-146a	BMP pathway	miR-146a exerts its repressive effect on *Drosophila* mothers against decapentaplegic protein 4 (SMAD4) through interacting with 3′-untranslated region (3′-UTR) of SMAD4 mRNA which is an important co-activator in the BMP signaling pathway	ADSCs	Xie et al. (2017)

miRNAs	Pathway	Related signaling pathways	Cell types	References
miR-148a-3p	Nrf2 pathway	miR-148a-3p negatively regulates p300 expression in osteoblasts by binding to the 3-UTR of p300 mRNA, which could inactivate the Nrf2 pathway, consequently down regulating RUNX2\ALP activity, and blunting osteoblast differentiation and subsequent bone reconstruction, ultimately leading to osteoporosis	osteoblastics	Wang et al. (2013); Liu and Sun, (2021)
miR-148b	BMP pathway	miR-148b directly targets *NOG*, whose gene product (noggin) is an antagonist to BMPs and negatively regulates BMP-induced osteogenic differentiation and bone formation	rBMSCs	Li K.-C et al. (2017)
miR-187	BMP pathway	miR-187 downregulates human BarH-like homeobox 2 (BARX2) through targeted regulation, inducing osteogenic differentiation of hMSCs. (33550149) Barx2 regulates the expression of several genes encoding cell-adhesion molecules and extracellular matrix proteins, including NCAM and collagen II (Col2a1) in the limb bud. Two members of the BMP family that are crucial for chondrogenesis, GDF5 and BMP4, regulate the pattern of Barx2 expression in developing limbs. Barx2 acts downstream of BMP signaling and in concert with Sox proteins to regulate chondrogenesis. Meech et al. (2005)	hMSCs	Zhang J et al. (2021)
miR-199a-5p	HIF1α-Twist1 pathway	At early stage of differentiation, hypoxia induces HIF1a-Twist1 pathway to enhance osteogenesis by up-regulating miR-199a-5p, while at late stage of differentiation, miR-199a-5p enhances osteogenesis maturation by inhibiting HIF1α-Twist1 pathway. And Runx2 might be negatively regulated by HIF1α, which is the direct target of miR-199a-5p	hMSCs	Chen X et al. (2015)
miR-200c	Wnt/β-catenin pathway	miR-200c overexpression is shown to downregulate SRY (sex detg. region Y)-box 2 (Sox2) and Kruppel-like factor 4 by directly targeting 3′-untranslated regions and upregulate the activity of Wnt signaling inhibited by Sox2	hBMSCs	Akkouch et al. (2019)
	BMP pathway	miR-200c effectively inhibits Noggin, an antagonist of BMP signals, by directly targeting the 3′UTR of Noggin	human embryonic palatal mesenchyme (HEPM)	Hong et al. (2016)
miR-205	Notch signaling pathway	miR-205 targets the 3′-untranslated region (UTR) of cfa-NOTCH2, which is a unique transcription regulator in bone angiogenesis. Inhibit miR-205 increases NOTCH2 expression, resulting in the elevated secretion of VEGF proteins and thereby stimulating angiogenesis and osteogenesis within the skeletal system	endothelial colony-forming cells (ECFCs)	Jiang et al. (2021)
miR-214	BMP pathway	miR-214 targets the 3′-UTR of the transcription factor ATF4 to inhibit bone formation. There is a runt-related transcription factor 2 (Runx2) binding site in Atf4 promoter Wang et al. (2013)	preosteoblast cells (MC3T3-E1 cells)	Wang Y et al. (2021)
	Pten/Pl3k/Akt pathway	miR-214 targets the 3′-UTR of phosphatase and tensin homolog (Pten). It has been demonstrated that Pten regulates RANKL-induced osteoclast differentiation from RAW 264.7 osteoclast precursors through Pl3K/Akt pathway	Osteoclasts	Zhao et al. (2015)
miR-222	Wnt/β-catenin pathway	miR-222 promotes neural differentiation of hBMSCs *in vitro* by targeting Nemo-like kinase (NLK) and decreasing NLK protein level. NLK is an inhibitor of Wnt/β-catenin signaling, which plays as a vital role in neuronal differentiation	hBMSCs	Lei et al. (2019)
	TGFβ pathway	Anti-miR-222 enhances *in vivo* ectopic bone formation through targeting to the 3′UTR of cyclin-dependent kinase inhibitor 1B (CDKN1B), a cell-cycle inhibitor Chang et al. (2018). CDKN1B regulate osteoblast differentiation through cell-cycle arrest, and cell-cycle arrest is a prerequisite for differentiation	hMSCs	Chang et al. (2018)
	STAT5A signaling pathway	MiR-222 was found to negatively modulate angiogenesis by targeting the c-Kit receptor Mazziotta et al. (2021) together with the signal transducer and activator of transcription 5A (STAT5A) Zhang Y et al. (2021). The c-Kit receptor is the receptor for the angiogenic activity of stem cell factor (SFC), and is expressed on the surface of ECs Mazziotta et al. (2021). STAT5A activates bFGF and IL-3, which in turn trigger vascular EC morphogenesis	hMSCs	Yoshizuka et al. (2016)

TABLE 2 | (*Continued*) The mechanism of miRNAs tested *in vivo* regulating osteogenic differentiation.

miRNAs	Pathway	Related signaling pathways	Cell types	References
miR-335-5p	Wnt/β-catenin pathway	in the STAT5A signaling pathway Zhang J et al. (2021). The present study demonstrated that although the target genes of miR-222 related to angiogenesis were not validated, down-regulation of the c-kit receptor and STAT5A by the miR-222 inhibitor might contribute to the enhanced neovascularization at the fracture site MiR335-5p may inhibit Wnt antagonist Dickkopf-1 (DKK1) expression and upregulate the Wnt pathway, promoting osteogenesis and angiogenesis as well as enhancing bone regeneration in steroid-associated osteonecrosis (SAON)	BMSCs	Li et al. (2022); Sui et al. (2018)
miR-467g	Ihh/Runx-2 signaling pathway	miR-467g targets the 3′-UTR of Runx-2, and down regulates Runx-2, inhibiting osteoblast differentiation	osteoblast	Kureel et al. (2017)
miR-590-5p	BMP pathway	The 3′-untranslated region of Smad7 was directly targeted by miR-590-5p. Smad7 inhibits osteoblast differentiation *via* Smurf2-mediated Runx2 degradation.miR-590-5p promotes osteoblast differentiation by indirectly protecting and stabilizing the Runx2 protein by targeting Smad7 gene expression Vishal et al. (2017)	mMSCs	Brenner et al. (2021)
	Wnt/β-catenin pathway	miR-590-3p binds to 3′UTR of APC mRNA. miR-590-3p can promote osteogenic differentiation *via* suppressing APC expression and stabilizing β-catenin	hMSCs	Wu S et al. (2016)
miR-672	TGFβ pathway	miR-672 negatively regulated the expression of TIMP2 by interacting with 3′-UTR of TIMP2 mRNA, regulating ADSCs angiogenesis *in vitro*. TIMP2, a member of the TIMP family, regulates the proteolytic activity of matrix metalloproteinases (MMPs), a group of proteolytic enzymes, and maintain the balance between extracellular matrix (ECM) breakdown and synthesis	ADSCs	Chen et al. (2021)
miR-2861	BMP pathway	MiR-2861 bound to the amino acid coding sequences (CDSs) of histone deacetylase 5 (HDAC5) mRNA with complementarity to the miR-2861 seed region, inhibiting the expression of HDAC5 protein at the translational level, thereby upregulating the expression of the runt-related transcription factor 2 (Runx2) protein and ultimately promoting the osteogenic differentiation of BMSCs	BMSCs	Li Z et al. (2021)
miR-5106	Wnt/β-catenin pathway	miR-5106 targets and increases Sox9 transcription factor activity Xue et al. (2017). Sox9 negatively regulates Runx2 and type X collagen expression to modulate endochondral ossification-related disorders Ding et al. (2021)	BMSCs	Xue et al. (2017)

2 APPLICATION OF DIFFERENT NONVIRAL VECTORS

2.1 Calcium Phosphates as Nonviral Vectors

Calcium phosphate (CAP) has long been used as a nonviral gene delivery vector. Calcium phosphate precipitates oligonucleotides on cells, and the precipitate is adsorbed on the cell membrane. Cells take up oligonucleotides along with the natural calcium uptake (Ruedel and Bosserhoff, 2012). Among all CAP materials, hydroxyapatite (HA) remains the most frequently used CAP to date. In addition, amorphous calcium phosphate, beta tricalcium phosphate, and dicalcium phosphate dihydrate are promising (Levingstone et al., 2020). Calcium phosphate nanoparticles present good binding affinity for RNA molecules; CAP nanoparticles have good osteoinduction, osteoconduction (Levingstone et al., 2020), biocompatibility, and

biodegradability, and they are nontoxic and nonimmunogenic (Bakan, 2018). Compared to cationic lipids, CAP nanoparticles show improved cytocompatibility, and spherical CAP nanoparticles increase osteoblast proliferation and osteogenic gene expression. However, the disadvantage of CAP nanoparticles is that the transfection efficiency of CAP is lower than that of viral vectors. Currently, surface functionalization, such as functionalization with cationic polymers, natural polymers, cell-penetrating peptides, biodegradable lipids, and polyethyleneimine/poly(ethylene) glycol, has been shown to improve cellular uptake and increase transfection efficiency (Levingstone et al., 2020). In addition, calcium phosphate material itself also promotes osteogenesis. Ca^{2+} and PO_4^{3-} play an important role in regulating bone resorption and bone deposition. Ca^{2+} induces the chemotaxis of monocytes, osteoblasts, and hematopoietic stem cells to the injury site, and it induces osteoblast

TABLE 3 | The information of miRNA transfection vectors applied to bone tissue engineering.

Types of vector	Transfection agent	Loading methods and loading efficiency	Unloading	Stability	Cells	Cellular uptake	Cytotoxicity	miRNAs	References
Nucleic acids	sticky-end tetrahedral framework nucleic acids (stFNAs)	complementary base pairing	RNase H cuts	degradation in >0.8 U ml⁻¹ RNase A, still existed at 35% FBS	BMSCs	the BMSCs had adsorbed a large amount of stFNA after 12 h	decreased cell viability when concentration >300 nm, altered cell viability only when carrying 2000 nm miR	miR-2861	Li S et al. (2021)
	tetrahedral DNA nanostructures (TDNs)	complementary base pairing	--	--	BMSCs	≈37.6% of BMSCs absorbed MiR@TDNs	--	miR-335-5p	Li et al. (2022)
Calcium phosphates	collagen-hydroxyapatite (coll-HA)			extending its half-life	rMSCs	55.4 ± 9.76% and 10.8 ± 6.37% at 3 and 7 days respectively		antagomiR-133a	Castaño et al. (2020); Mencía Castaño et al. (2016)
	nanohydroxyapatite (nHA) particles	electrostatic interaction Bose and Tarafder, (2012)	CaPs dissoluted in the acidic environment of the endocytic vesicle Bose and Tarafder, (2012)		hMSCs	precipitates at the cell surface and undergo endocytosis, 33.5 ± 1.5% and 39.6 ± 4.7% respectively for the 10 and 20 nM doses Dy547 nanoantagomiR by day 3 Bose and Tarafder, (2012); Mencía Castaño et al. (2015)	no cytotoxic effects	antagomiR-16	Mencía Castaño et al. (2019)
Nano systems	Layered double hydroxide (LDH) nanoparticles	electrostatic interactions with mild orbital agitation	proton sponge effect	protective effect of LDH against serum degradation	BMSCs	clathrin-mediated endocytosis, the buffering capacity facilitates endosomal escape, internalization was increased in 24 h	did not remarkably affect cell proliferation at any concentration tested	miRNA let-7d	Yang K et al. (2021)
	mesoporous silica nanoparticles (MSN)	miR222 filled the pores of MSNs, optimal loading capacity: around 6.6 wt% (MSN:miR222 = 15:1)	disulfide bonds will break up by glutathione (GSH), 15% released on the first day, and 80% at the end of 35 days	disulfide bonds and amino groups to stabilize miR222, release <3% after 3 days in phosphate-buffered saline (PBS)	hBMSCs	endocytos	non-toxic	miR-222	Lei et al. (2019)
	CTH nanoparticle (chitosan solution (CS), Sodium tripolyphosphate (TPP), hyaluronic acid (HA))	The loading efficiency was over 90% when the N/P ratio was 15:1	40–50% at 21 days		murine BMSCs	reached to the greatest transfection efficiency with 2 mM CTH-antagomiR-133a/b	did not impair BMSCs proliferation and exhibited no cytotoxicity in BMSCs	antagomiR-133a/b	Jiang et al. (2020)
	(hydroxypropyl) cellulose (HPC)-modified silver nanoparticles (SNPs)	a nitrobenzyl photocleavable linker between the 3' terminal and miR-148b sequence, NP ratio: 5000:1	405 nm irradiation		rBMSCs	56.1 ± 2.2% of cells contained SNP-miR148b-TAMRA 12 h post-transfection, just before illumination. After photo-activation, the percentage decreased	no any major inhibition on the proliferation of rBMSCs	miR-148b	Moncal et al. (2019)
	dual-sized pore structure calcium-silicon nanospheres (DPNPs)	coordination bond formation between calcium ions in the DPNPs and phosphate in miR-210, miR-210 could be adsorbed on the surface of the mesoporous structure of DPNPs	reaches maximum releasing amount after 4 days	the electrophoretic bands can be detected even after 10 h	mBMSCs	79.20%	no any mass cell death	miR-210	Liu et al. (2021)
	PLLA/polyethylene glycol (PEG) co-functionalized mesoporous MSN, poly (lactic acid- co-glycolic acid) microspheres (PLGA MS)	electrostatic interactions between an amino-functionalized multi-armed cationic polymer and miR	90% by day 50 at 260 nm		mice T cells	the cationic polymer can bind and transfer the miRNA into T cells	no inhibitory effect on T cells	miR-10a	Liu et al. (2019b)
	chitosan/tripolyphosphate/ hyaluronic acid/antimiRNA-138 nanoparticles (CTH/antimiR-138 NPs)	ionic gelation and encapsulation of miR	26.8% in the first 2 d, and 52.4% by 21 d		rMSCs			antimiR-138	Wu et al. (2018)
	chitosan nanoparticles	electrostatic interactions, 82%	About 30%, 55% and 65% within 7, 14 and 21 days, respectively	nanoparticle/agomir complexes showed constant expression of miRNA in long-term culture	hMSCs	Chitosan binding to negatively charged cellular membranes can enhance cellular uptake	no significant cytotoxicity	agomiR-199a-5p	Chen X et al. (2015)

TABLE 3 | (Continued) The information of miRNA transfection vectors applied to bone tissue engineering.

Types of vector	Transfection agent	Loading methods and loading efficiency	Unloading	Stability	Cells	Cellular uptake	Cytotoxicity	miRNAs	References
	electrospun polycaprolactone (PCL) nanofibers		>50% in the first 72 h, release sustained up to 14 days		induced pluripotent stem cells (iPSCs)		iPSCs showed an increasing proliferation trend	miR-22 and miR-126	Tahmasebi et al. (2020)
	bioactive glass nanoparticles (BGNs) silica nanoparticles (SNs) polyethylenimine (PEI)	SNs: physical adsorption, BGNs: a strong surface interaction, BGNs showed a higher miRNA binding amount (~200 μg/mg) at 40–320 μg/ml nanoparticle concentrations compared to that of SNs (~20 μg/mg)	miRNA was released from BGNs after degradation	>82% of the intact miRNA left after 3 h of incubation in 25% FBS, in BGN/miRNA and PEI/LIPO groups, while almost completely degraded in SN/miRNA group	BMSCs	BGN group: ~45%, PEI: 35%, LIPO: 35%	live cell attachment: BGNs group: good at 30–240 μg/ml, PEI 25K and LIPO groups: significantly low; cell viability: significantly higher with 30 and 60 μg/ml BGNs after 72 h	miR-5106	Yu et al. (2017)
	monodispersed BGNs with polyethylenimine (PEI)	a strong binding affinity bwteen the Ca2+ in BGs framework and the phosphates groups in miRNA		>80% of the intact miRNA after 24 h nuclease incubation, but only 50% and 35% in BGN and Lipo group	BMSCs	BGNCs group: 45.3%, BGNs group: 40.1%, Lipo group: 35.1% (after 48 h)	good cells attachment morphology, no dead cells after 1 d	miR-5106	Xue et al. (2017)
	chitosan/hyaluronic acid nanoparticles (CS/HA NPs)	electrostatic interactions, N/P ratio was 20:1	release sustained up to 14 days		hBMMSCs	a moderate and long-lasting transfection process up to 14 days	no any obvious cytotoxicity after 24 hours	miR-21	Wang et al. (2016)
	chitosan (CS)/ tripolyphosphate (TPP)/ Hyaluronic Acid (HA) nanoparticles (CTH NPs)	electrostatic interactions, N/P ratio >20:1	losing the tight binding between the gene and the carrier, and prolong circulation time of the delivery system by reducing their non-specific interactions with serum proteins	With N/P ratio increasing, the antimiR-138 in complexes was subject to less RNase degradation	rMSCs	40% to nearly 70% with the antimiR-138 concentration from 50 to 150 nM	no toxicity	antimiR-138	Wu G et al. (2016)
	polyethylenimine (PEI) bound to magnetic nanoparticles (MNPs)	a salt-induced aggregation called "magnetofection"	Released the DNA in the perinuclear region due to strong biotin-streptavidin connections of MNPs. Delyagina et al. (2011)	Appropriate condensation of miR protects miR from early enzymatic degradation	hMSCs	miR/PEI/MNP group (N/P ratio of 2.5): 79%, miR/PEI/CombiMag: 56%, miR/ Magnetofectamine: 75%	no significant cell mortality	miR	Schade et al. (2014)
	photocleavable (PO) silver nanoparticle	The light activated technology links a truncated single stranded miRNA to SNP surface via a PC linker	PC linker release miRNA from the particle by a discrete photo-trigger	The HPC was displaced with negatively charged PC-miR-148b, increasing colloidal stability in aqueous solution	hASCs		minimal cytotoxicity (90.08 ± 2.12% viable hASCs	miR-148b	Qureshi et al. (2013)
	gold nanoparticles	miR can be attached to the gold nanoparticle			hMSCs	At 1 h GNPs were mainly at the cell periphery, whilst at 48 h the NPs were within the cell, mainly packaged into endosomes	no adverse effects	antagomiR-31	McCully et al. (2018)
	PEI-capped gold nanoparticles (AuNPs)	electrostatic interactions		stable in serum for 6 h	hMSCs and MC3T3-E1 cells	AuNPs/Cy3-miR-29b: 54 ± 0.71% and 88 ± 1.42% for hMSCs and MC3T3-E1 cells, lipo/miR-29b: 65.12 ± 1.85% and 80.57 ± 1.77%	no significant cytotoxicity, lower toxicity than lipo	miR-29b	Pan et al. (2016)
	GNP SNP	A stable covalently bound linker, amide bond, conjugated molecular cargo to surfaces	photothermal release at temperatures ≥60°C or at ≈400 nm irradiation	the 2'-O-methyl modified RNA mimics prolonged the lifetime of RNA in serum	hASCs		toxic cellular response to the 405 nm LED light source	miR-148b and miR-21	Abu-Laban et al. (2019)
	lyophilized mesoporous silica nanoparticles with core-cone structure and coated with polyethylenimine (MSN-CC-PEI)	electrostatic attraction, the loading efficiency achieved 60% with 40 μg/ml nanoparticles	proton sponge (proton buffering)		rBMSCs		considerably more cytotoxicity at 40 μg ml⁻¹ PEI coated particles, no significant cytotoxicity in uncoated particles, the optimal exposure conditions for the PEI coated NPs would be less than 24 h	mo-miRNA-26a-5p	Hosseinpour et al. (2021)
	MSNs-PEI-KALA peptide	miR-26a is bonded to the MSN surface	KALA's membrane disrupting activity	no release of miRNA in RNase A	rBMSCs	~23% fluorescence intensity at 12 h with 20 μg/ml complexes	no significant cytotoxicity	miR-26a	Yan et al. (2020)
	lipidoid nanoparticles	electrostatic interactions			mBMSCs		no significant cytotoxicity	miR-335-5p	Sui et al. (2018)

TABLE 3 | (Continued) The information of miRNA transfection vectors applied to bone tissue engineering.

Types of vector	Transfection agent	Loading methods and loading efficiency	Unloading	Stability	Cells	Cellular uptake	Cytotoxicity	miRNAs	References
	R9-LK15 nanocomplexes	electrostatic interactions		stable in serum for up to 24 h	rBMSCs	a similar or higher transfection efficiency than Lipofectamine 2000 / R9-LK15/miR-29b nanocomplexes: 78.33% ± 5.90, Lipo/miR-29b nanocomplexes: 36.43% ± 1.75	no significant cytotoxicity, much less cytotoxic than Lipo	miR-29b	Liu Q et al. (2019)
	nanocapsules and O-carboxymethyl chitosan (CMCS) powder mixed gel	electrostatic interactions	a fast release within the first 20 h (~50%), ~10% remained in the coating after 100 h		MSCs		good biocompatibility	miR-21	Geng et al. (2020)
	N-(3-aminopropyl) methacrylamide, acrylamide and ethylene glycol dimethacrylate nanocapsules	electrostatic interactions, hydrogen bonding, free-radical polymerization wraps the miRNA molecules with thin shells of network polymer Liu et al. (2015)	The crosslinker molecules are degradable in acidic environment (pH 5.4) Liu et al. (2015)	no extraction of As-miR-21 by heparin from the nanocapsules, better stability against RNase and serum than lipo/AS-miR-21 Liu et al. (2015)	Osteoblast-like MG63 cells	two and fivefold higher than that of lipo/AS-miR-21 Liu et al. (2015)	no any obvious rejection phenomenon 1 month after surgery Geng et al. (2018), low cytotoxicity Liu et al. (2015)	miR-21	Geng et al. (2018)
	CMCS nanocapsules	electrostatic interactions, hydrogen bonding, free-radical polymerization wraps the miRNA molecules with thin shells of network polymer		no extraction from nanocapsules by heparin, compared to the lipo/miR-21 complex	hUMSCs	61.6% after 48 h (nearly 3.6-fold that of the CMCS/lipo/miR-21 group), 1.6-fold greater at 3 days	97.6 ± 9.3% cell viability at a miR-21 concentration of 50 nM	miR-21	Meng et al. (2016b)
	CMCS coating nanocapsules					77.14% cells presented green fluorescence after 4 h of incubation, while 67.56% in lipo2000 group	78.28% hUMSCs viability at the nanocapsule concentration of 500 nM, and 93.05% at 50 nM	miR-29b	Meng et al. (2016a)
	nanocapsules	Electrostatic interaction and hydrogen bonding interaction formed a polymer shell around the miR-21			rMSCs	high efficiency	increased cytotoxicity when concentration >100 nm, metabolic activity was 98.06% at 50 nm	miR-21	Sun et al. (2020)
Liposomes	aspartate, serine, serine (AspSerSer)6-liposome				osteoblasts			mir-133a	Zhou et al. (2021)
	Lipofectamine 3000 Lipofectamine 2000				hASCs, rBMSCs, hBMSCs, rabbit BMSCs			miR-33a-5p, miR-34a, miR-106a Inhibitor, antimiR-222, antimiR-138, miR-93-5p inhibitor	Shen et al. (2020) Liu H et al. (2019); Sun et al. (2018); Chang et al. (2018); Yan et al. (2014); Zhang Y et al. (2021)
	Lipofectamine RNAi MAX Carthew et al. (2020)		Complexes gradually diffused, with full release taking ~7 days Carthew et al. (2020)		MCO cells	transfection efficiency: 97% Carthew et al. (2020)		antimiR-467g	Kureel et al. (2017)
	siPORT NeoFX transfection agent		proton sponge		hBMMSCs, mBMMSCs, ADSCs			miR-26a, anti-hsa-miR-221	Li et al. (2013); Hoseinzadeh et al. (2016)
	X-tremeGENE transfection reagent				mBMSCs, mMSCs			miR-590-5p, miR-590-5, miR-15b	Balagangadharan et al. (2018); Vishal et al. (2017); Vimalraj et al. (2016)
Other types	injectable poly (ethylene glycol) (PEG) hydrogel Carthew et al. (2020)	covalently connected by an ultraviolet (UV) light-cleavable linker	The release rate was ~70% upon 365 nm UV irradiation for 5 min	no miR-26a release in the absence of UV irradiation	hMSCs	The internalization efficiency was about 60% in 1 day	The biocompatibility of the gel are suitable for the surface-cultured cells	miR-26a	Gan et al. (2021)
	poly (ethylene glycol) (PEG) hydrogels				hMSCs			miR-20a	Nguyen et al. (2018)
		electrostatic interactions			BMSCs			miR-26a	Li et al. (2020)

TABLE 3 | (Continued) The information of miRNA transfection vectors applied to bone tissue engineering.

Types of vector	Transfection agent	Loading methods and loading efficiency	Unloading	Stability	Cells	Cellular uptake	Cytotoxicity	miRNAs	References
	a comb-shaped polycation (HA-SS-PGEA) consisting of Hyaluronic acid (HA), disulfide groups and ethanolamine (EA)-functionalized poly (glycidyl methacrylate) (PGMA)		DL-dithiothreitol (DTT) induced disulfide bond cleavage; Burst release in first 3 days, and sustained release for 1 month	The HA-SS-PGEA completely retarded miRNA migration at the N/P ratio of 1 and enabled NPs stable to resist anionic macromolecules to prevent premature failure of miRNA.		The ability of HA-SS-PGEA to transport miRNA through cellular membrane is stronger than PEI and PGEA.	The cell viability reached above 90%		Li X et al. (2017)
	Bio-inspired bioactive glasses	The miR-7-FAM labelling efficiency >90% when the PBGs-NH2/microRNA ratio was 40 or 80			human Hela cell line	>90% after 4 h incubation	The cells were not in a good state and many of them became irregular when ≥100 μg ml−1, although the positive expression rate was still >95%	miR-7	
	zinc(II) quercetin complexes (Zn + Q (PHt)) (BMC)				MG-63 cells		no declined cytocompatibility till >60 μM	pre-miR-15b	Raj Preeth et al. (2021)
	Ascorbic Acid-PEI Carbon Dots (CD)	electrostatic interactions, miR-2861 fully complexed with the CD at a 4:1 weight ratio of the CD and miR			BMSCs	Cellular uptake had started before 5 min and exponentially boosted with time before 4 h and then became slow and plateau phases/saturation; transfection efficiency: 47.44%	With the increase of PEI concentration, the viability of BMSCs reduced remarkably, only 35.00% at 50 μg/ml; no significant cytotoxicity of CD	miR-2861	Bu et al. (2020)
	PEI	electrostatic interactions			hMSCs	endocytosis, transfection efficiency: 79% (4 kDa PEI) and 77% (40 kDa PEI)	no significant cytotoxicity	miR-100-5p, miR-143-3p, miR-20a	Carthew et al. (2020); Huynh et al. (2016); Nguyen et al. (2014)
	PEI-functionalized graphene oxide (GO) complex	electrostatic interactions; At the N/P ratio of 30 (**Figure 3D**), GPM complex would wrap miR-inhibitor inside and prevent it being degraded		RNase A have no influence on the GFP RNA delivered into cells	mouse osteoblastic cells (MC3T3-E1)	cell uptake and transfection efficacy for 24 h greater than naked miR-inhibitor or Lipofectamine 2000 groups	no significant toxicity	miR-214 inhibitor	Ou et al. (2019)
	silk-based orthopedic devices, Xfect RNA Transfection Reagent	electrostatic interactions	initial release of ~20% in the first 24 h, the continued release of an additional 42% in the next 48 h, an additional 36% after 168 h		hMSCs	Cells are typically transfected within 24 h and have bioactivity up to 2 or 3 weeks	significantly higher cell viability after 72 h and 7 days, no clear difference in morphology, no apoptotic	antimiR-214	James et al. (2019)
	Low molecular weight protamine (LMWP)	electrostatic interactions		no degradation in serum for up to 24 h	hMSCs	6.5-fold transfection efficacy than the cationic lipids in 5 h	no significant change in the viability of hMSCs, mild toxicity (around 14%) in liposomal group	miR-29b	Suh et al. (2013)
	Electrospinning of gelatin	The miRNA was loaded uniformly throughout the fibers	an initial burst followed by sustained release for up to 72 h		MC3T3-E1 osteoblast-like cells		no significant differences in cell viability after 24 h	miR-29a inhibitor	James et al. (2014)
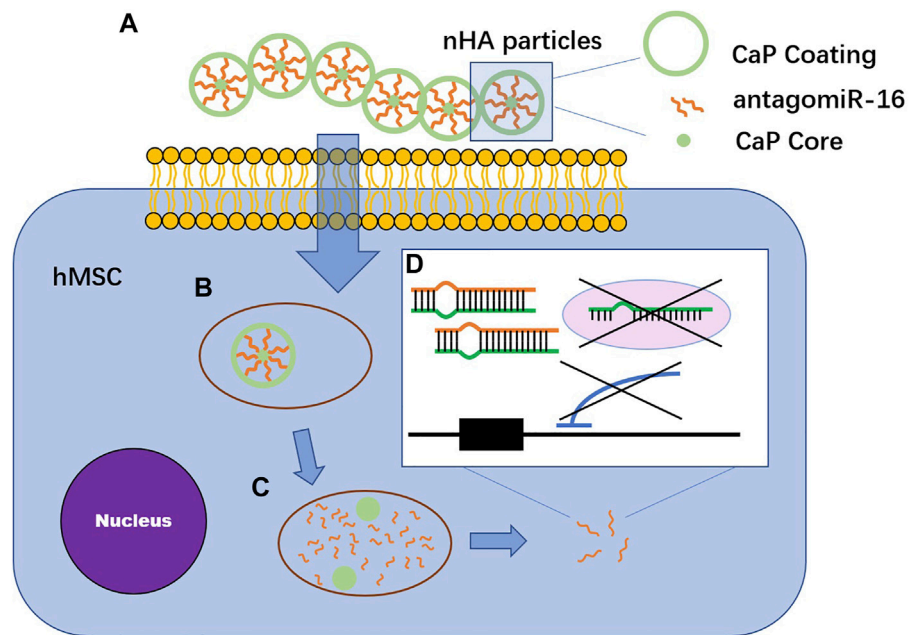
FIGURE 3 | The mechanism of calcium phosphates vectors transfecting antagomiR-16. **(A)** AntagomiR-16 binds to nHA particles through electrostatic interaction between Ca^{2+} in CaP vector and phosphate groups in miRNA structure. The complex are found in multiparticulate formations. **(B)** nHA-antagomiR-16 particles pass through lipid bilayer cell membranes along endocytosis. **(C)** AntagomiR-16 undergoes endosomal escape before the fusion of endosome with lysosome. **(D)** AntagomiR specifically complement to their mature target miRNA, inducing the repression of miRNA, preventing translation repression or Smad5 and AcvR2a mRNA degradation *via* RISC.
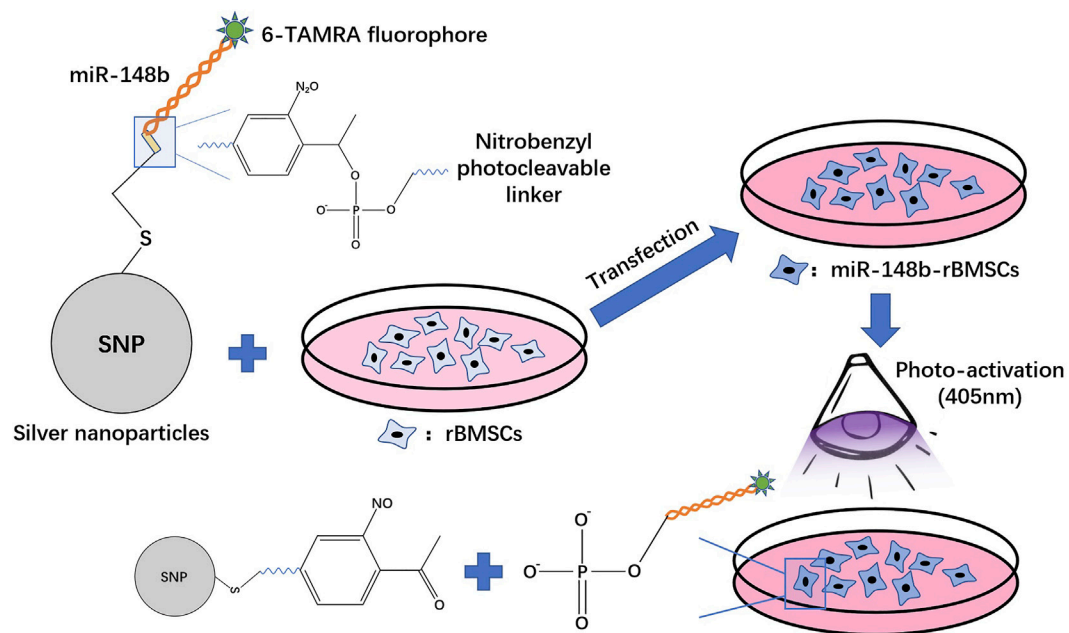
FIGURE 4 | The procession of silver nanoparticles (SNPs) with a nitrobenzyl photocleavable group transfecting miR-148b into rBMSCs.

proliferation, osteoblast differentiation, and osteogenic gene expression. PO_4^{3-} participates in the proliferation and differentiation of osteoblasts by entering the mitochondria and

stimulating the production of adenosine triphosphate (ATP), which is converted to adenosine and promotes osteogenesis (Levingstone et al., 2020).

Irene et al. combined nanohydroxyapatite (nHA) particles with collagen-nHA scaffolds to deliver antagomiR-16 to human bone mesenchymal stem cells (hMSCs). The levels of Runx2 (the key transcription factor for osteogenesis) and osteocalcin as well as the mineral calcium deposition of hMSCs were significantly increased, indicating the bone repair potential of the combination (Mencía Castaño et al., 2019) (**Figure 3**). Castaño et al. implanted collagen-nanohydroxyapatite (coll-nHA) scaffolds without cells into calvarial defects of rats to deliver antagomir-133a; 1 week after implantation, antagomir-133a began to be released at the implantation site, and the bone repair volume was ten times that in the negative control group after 4 weeks, indicating that the platform accelerates bone repair *in vivo* without the participation of exogenous cells (Castaño et al., 2020). This system did not inoculate cells before implantation because recent studies have emphasized that adding cells to scaffolds is a limiting factor in the field of tissue engineering (Zhang et al., 2016). Coll-nHA has been demonstrated to be both a nonviral vector and a scaffold (Curtin et al., 2015).

2.2 Nanosystem as a Nonviral Vector

Nanotransfection materials mainly include nanoparticles and nanocapsules. Nanoparticles are structures with a size (1–100 nm) similar to that of biomolecules (protein, DNA, and RNA) (Rahim et al., 2018; Chiang et al., 2021). Nanoparticles covalently bind biomaterials, and the physicochemical properties of a variety of biomedical applications are met through surface modification (Kashapov et al., 2021). The types of nanoparticles commonly used for miRNA delivery applications include organic nanoparticles, such as lipid nanoparticles, as well as inorganic nanoparticles, such as metal nanoparticles and silica nanoparticles. Despite this classification, many inorganic and organic composite systems have been developed to achieve synergy (Pan et al., 2016; Kashapov et al., 2021). Because miRNAs are negatively charged, the nanoparticles are adjusted to be neutral or slightly negatively charged (Chiang et al., 2021; Kashapov et al., 2021).

Gold nanoparticles (GNPs) and silver nanoparticles (SNPs) are commonly used metal nanoparticles. In a previous study, researchers encapsulated antagomiR-31 with GNPs and delivered them to preosteoblastic and primary human mesenchymal stem cells (hMSCs) *in vitro*, which resulted in increased osterix protein and osteocalcin in the 2 cell types, indicating cell osteogenesis (McCully et al., 2018). Pan et al. combined polyethyleneimine (PEI)-capped gold nanoparticles with miR-29b, which effectively entered hMSCs and mouse embryonic osteoblasts (MC3T3-E1 cells), promoting the expression of alkaline phosphatase (ALP), the early-stage osteogenic gene, and medium-stage marker Runx2 as well as the expression of OCN and OPN, the late-stage osteogenic differentiation markers. Moreover, the combination showed negligible cytotoxicity (Pan et al., 2016). Moncal et al. synthesized (hydroxypropyl) cellulose (HPC)-modified SNPs and functionalized them with photolytic miR-148b. miR-148b mimics were photoactivated at wavelengths ranging from 350 to 450 nm, causing them to be released from the surface of SNPs. The proliferation rate of rat bone marrow-derived mesenchymal stem cells (rBMSCs) transfected with miR-148b was significantly higher than that of the control group. Calvarial defects in rats were almost completely repaired (Moncal et al., 2019) (**Figure 4**). Abu-Laban et al. cotransfected human adipose stem cells (hASCs) with SNP-miR-21 and GNP-miR-148b and activated the constructs at wavelengths of 405 and 503 nm; they reported that the degree of cell mineralization in the cotransfection group was higher than that in the group treated with one particle alone (Abu-Laban et al., 2019).

There are many other inorganic nanoparticles as well as the calcium phosphate nanoparticles mentioned above. Through appropriate synthesis and functionalization technology, inorganic nanoparticles show unique optical, magnetic, and electrical properties as well as strong loading capacity, mechanical stability, controllable size, and controllable porosity (Yang K. et al., 2021; Kashapov et al., 2021). Mesoporous silica nanoparticles (MSNs), for instance, have many favorable properties, such as low toxicity, ideal degradability, flexible design, tunable size, and high porosity. Hosseinpour et al. and Yan et al. loaded the miR-26a simulant into MSNs and delivered the complex to rBMSCs. miRNA stably bonded to the surface of nanoparticles *via* electrostatic attractions, and the carrier protected the miRNA from degradation by RNase A. The complex significantly enhanced osteogenic differentiation and extracellular matrix deposition and mineralization (Yan et al., 2020; Hosseinpour et al., 2021). Liu et al. constructed silica nanoparticles containing poly(lactic acid-coglycolic acid) (PLGA) microspheres (MSs). PLGA MSs release miR-10a, locally recruit T cells, and stimulate them to differentiate into Treg cells, mediating immunotherapy against bone loss in a mouse periodontitis model (Liu et al., 2018b). In addition, nanoparticles made of pinecone-like bioactive glasses have shown excellent apatite mineralization properties. After chemical modification of miR-7 to produce a miR-7-FAM complex, both the miRNA-loading efficiency and cell transfection efficiency of the complex are greater than 90% (Li X. et al., 2017).

The common organic material is chitosan, which has good aqueous solubility, good biocompatibility, controllable biodegradability, and strong bioactivity. Jiang et al. used CTH nanoparticles (chitosan solution, CS; sodium tripolyphosphate, TPP; and hyaluronic acid, HA) to transfect antagomiR-133a/b into murine BMSCs. The loading efficiency was over 90% when the N/P ratio was 15:1 and exhibited no cytotoxicity in BMSCs (Jiang et al., 2020). Chen et al. reported that approximately 30%, 55%, and 65% of agomiR-199a-5p was released within 7, 14, and 21 days, respectively, from chitosan nanoparticles, indicating that this transfection agent could continuously release miRNA in long-term culture (Chen X. et al., 2015). Another common organic material is polyethyleneimine (PEI), which is often combined with bioactive glass nanoparticles (BGNs) or MSNs. Xue et al. used monodispersed BGNs with PEI to transfect miR-5106 into BMSCs. The complex effectively protected miRNA from degradation, and more than 80% of the intact miRNA existed after 24 h of nuclease incubation compared to 35% in the Lipo group (Xue et al., 2017).
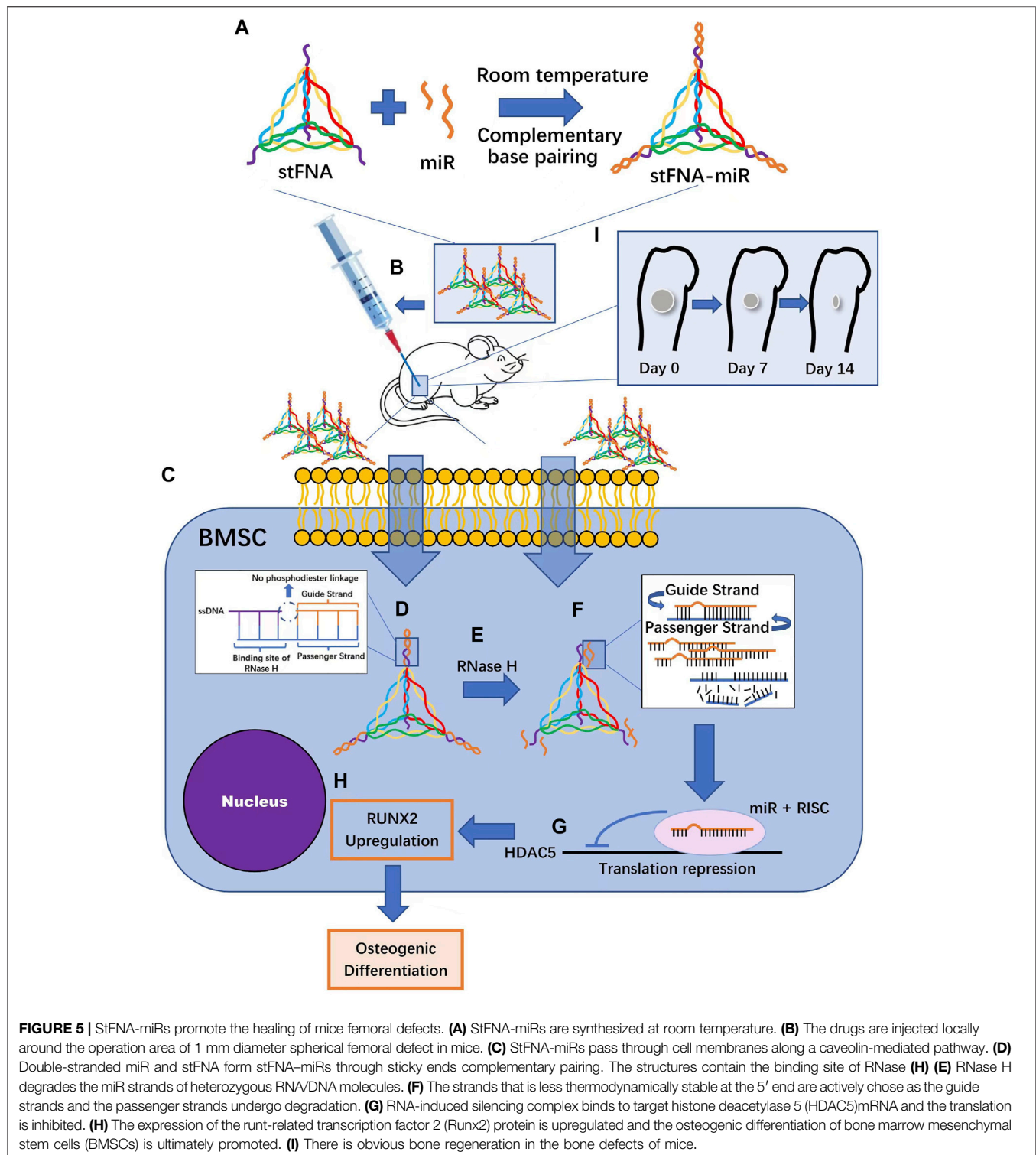
FIGURE 5 | StFNA-miRs promote the healing of mice femoral defects. **(A)** StFNA-miRs are synthesized at room temperature. **(B)** The drugs are injected locally around the operation area of 1 mm diameter spherical femoral defect in mice. **(C)** StFNA-miRs pass through cell membranes along a caveolin-mediated pathway. **(D)** Double-stranded miR and stFNA form stFNA–miRs through sticky ends complementary pairing. The structures contain the binding site of RNase **(H) (E)** RNase H degrades the miR strands of heterozygous RNA/DNA molecules. **(F)** The strands that is less thermodynamically stable at the 5′ end are actively chose as the guide strands and the passenger strands undergo degradation. **(G)** RNA-induced silencing complex binds to target histone deacetylase 5 (HDAC5)mRNA and the translation is inhibited. **(H)** The expression of the runt-related transcription factor 2 (Runx2) protein is upregulated and the osteogenic differentiation of bone marrow mesenchymal stem cells (BMSCs) is ultimately promoted. **(I)** There is obvious bone regeneration in the bone defects of mice.

The formation of nanocapsules begins with the enrichment of monomers and crosslinkers around miRNA molecules. Monomers and crosslinkers form polymer shells around miRNA molecules through *in situ* polymerization, thereby forming nanocapsules (Meng et al., 2016b). Meng et al. used O-carboxymethyl chitosan (CMCS) to encapsulate miRNA-21

mimics. CMCS provides protection for the miRNA from heparin and improves transfection efficiency to 61.6% after 48 h and by 1.6-fold at 3 days, significantly promoting the osteogenic differentiation of human umbilical cord mesenchymal stem cells (HUMSCs) and bone formation (Meng et al., 2016b). Sun et al. first designed a metalloproteinase-sensitive nanocapsule,

FIGURE 6 | The procession of ascorbic acid-PEI carbon dots (CD) transfecting miR-2861 into BMSCs.
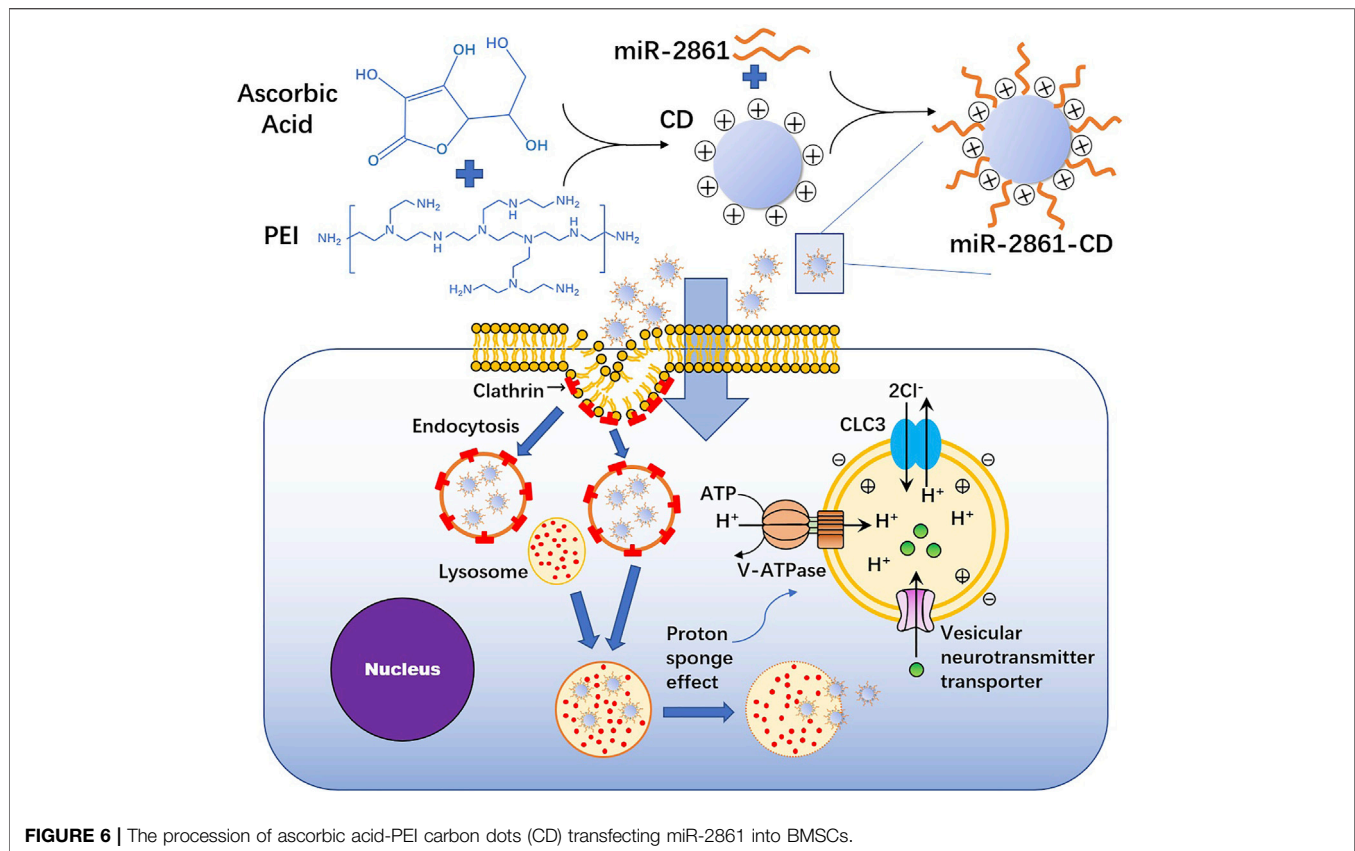
which was bound to the surface of miRNA-21 through *in situ* free radical polymerization; they mixed the miR-21/nanocapsule with CMCS until a gel material with good fluidity and injection was formed, and they applied the material to a rat fracture model to promote bone repair (Sun et al., 2020). Geng et al. used N-(3-aminopropyl) methylacrylamide, acrylamide, and ethylene glycol dimethacrylate nanocapsules to encapsulate miR-21 and delivered it to osteoblast-like MG63 cells, promoting the formation and mineralization of new bone (Geng et al., 2018). The nanocapsules showed more than twice the transfection capacity of commercial Lipofectamine transfectants (Liu et al., 2015).

2.3 Liposomes as Nonviral Vectors

Lipofection is an effective method to transfect miRNA into cells (Ruedel and Bosserhoff, 2012). In lipid transfection, microvesicular liposomes are formed by cationic lipids. The hydrophilic head of cationic lipids can condense with nucleic acids, and the hydrophobic tail of cationic lipids can form micelles or lipid bilayer structures arranged in spherical shell shapes to wrap the cargo in the middle (Goodwin and Huang, 2014; Carter and Shieh, 2015). When the liposome collides or attaches with the cell membrane, it fuses with the cell membrane or undergoes endocytosis to release the cargo (Carter and Shieh, 2015; Hori, 2019). A large number of commercial liposome transfection agents have been used in bone tissue engineering. It is convenient to use liposomes to study the effect

of miRNA or scaffolds on osteogenesis because liposomes have good biocompatibility, and researchers can easily functionalize the surface of liposomes to carry certain targeted ligands for cell recruitment or to anchor to scaffolds (Kang et al., 2021; Scheideler et al., 2020). In addition, because of the clear transfection effect of liposomes, they are now the control group in many studies of nonviral vectors. Lipofectamine RNAi Max transfection agent has become the gold standard of miRNA nonviral vectors, and its cell transfection efficiency has reached 97% (Carthew et al., 2020). Meng et al. used the CMCS/Lipofectamine 2000 complex as the positive control of CMCS powder to deliver miR-21 to hUMSCs. The results showed that the delivery efficiency of CMCS/n (miR-21) (61.6%) was approximately 3.6 times that of the positive control group (17.2%) (Meng et al., 2016b). Other scholars have used Lipofectamine 2000 as a control to verify that there is no significant cytotoxicity of R9-LK15 nanocomplexes to cells, which is lower than lipo (Liu Q. et al., 2019). In addition, lipid vectors also include stable nuclear acid lipid particles (SNALPs), solid lipid nanoparticles (SLNs), and pH-responsive lipids. SLNs are defined as colloidal drug carriers that are 50 nm to 1 μm in diameter (Mishra and Singh, 2020). SLNs with cations condense with anionic miRNA through electrostatic interactions to form SLN/miRNA complexes (Liu et al., 2016). The other two are mainly used in delivering siRNA and drugs. At present, there is no case of delivering miRNA in bone tissue engineering using these three vectors.

FIGURE 7 | Nonviral biomaterials for microRNA transfection in bone tissue engineering.
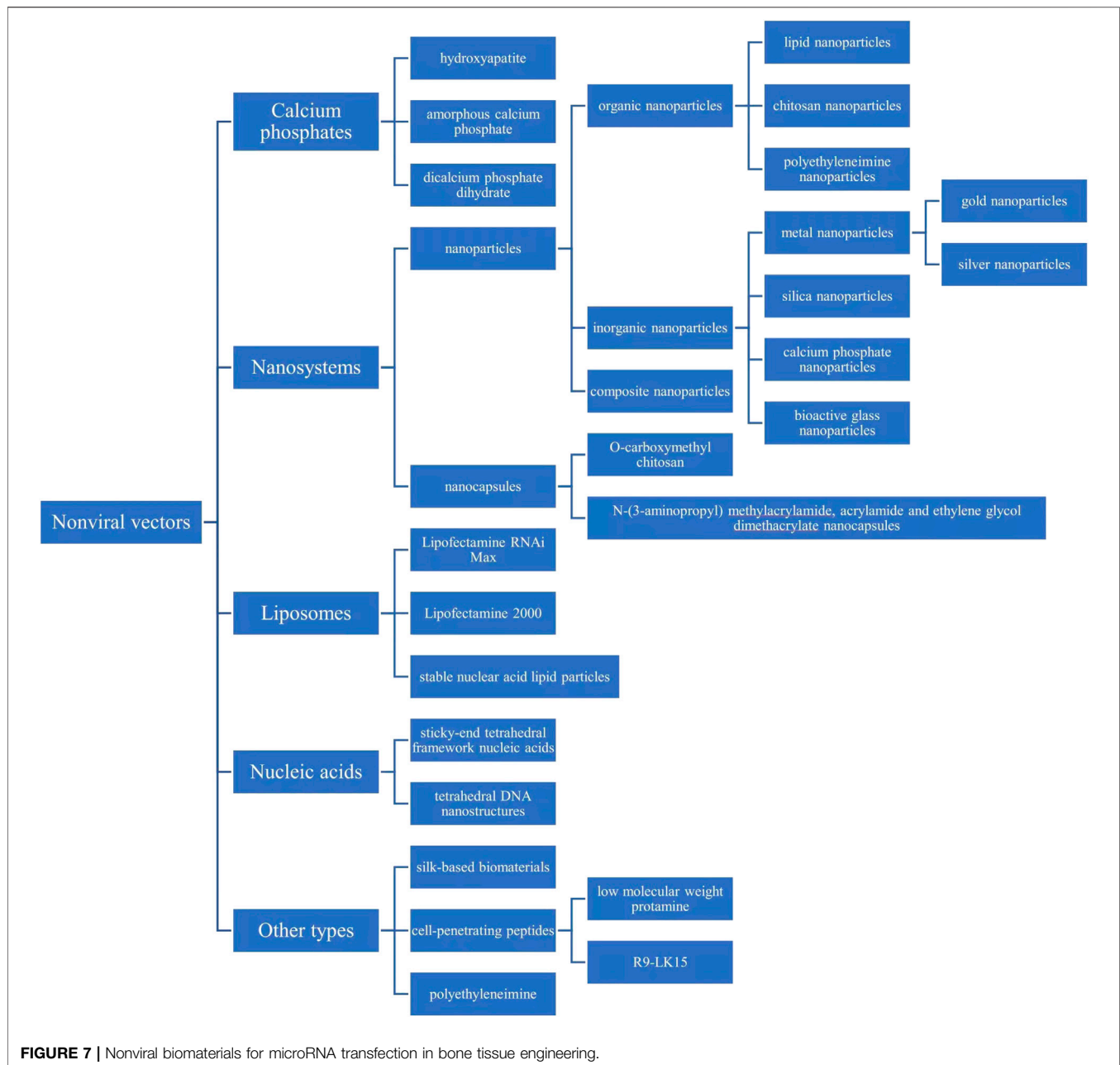
2.4 Nucleic Acids as Nonviral Vectors

Transporters based on nucleic acid structures have natural advantages, including high precision brought by Watson–Crick base pairing, structural predictability, good biocompatibility, simple manufacture, and high yield (Tian et al., 2020). Li et al. made sticky-end tetrahedral framework nucleic acids (stFNAs) that carry double-stranded miRNA, including a guide chain and a passenger chain with sticky ends. miRNA and stFNAs are combined by base complementary pairing. When the complex enters the BMSCs through the cell membrane, RNase H cuts the complex to unload miRNA (Li S. et al., 2021) (**Figure 5**). Li

et al. used tetrahedral DNA nanostructures (TDNs) to carry miR-335-5p (Li et al., 2022). TDNs have been demonstrated to have high mechanical stiffness, high stability and rich functional modification sites as well as to be able to carry siRNA, CGP, and miRNA (Zhang et al., 2018; Li et al., 2022).

2.5 Other Types of Materials as Nonviral Vectors

Other biomaterials that can be applied for miRNA delivery include silk-based biomaterials, cell-penetrating peptides, and PEI. Silk-based bioactive materials have attracted much

attention due to their good orthopedic repair ability (James et al., 2019). James et al. delivered antisense miRNA-214 (AS-miR-214), which inhibited the endogenous expression of osteoinductive antagonists *via* a silk-based orthopedic device. This device released miRNA continuously for 7 days, promoting osteogenic gene expression and increasing ALP levels and calcium deposition of hMSCs (James et al., 2019).

Suh et al. used a cell-penetrating peptide rich in arginine, called low molecular weight protamine (LMWP), whose transfection efficacy increased 6.5-fold that of the cationic lipids in 5 h. The LMW1/miR-29b complex enhanced the expression of ALP, OCN, OPN, and Runx2 as well as induced the differentiation of hMSCs into osteoblasts (Suh et al., 2013). Additionally, there is a new cell-penetrating peptide called R9-LK15. R9-LK15/miRNA-29b nanocomplexes maintained the stability of miR-29b in serum for up to 24 h. Moreover, the efficiency of R9-LK15 in delivering miR-29b to BMSCs was 10 times higher than that of Lipofectamine 2000. The complex promoted osteogenic differentiation and extracellular matrix mineralization of BMSCs by upregulating the expression of ALP and downregulating the expression of histone deacetylase-4 (Liu Q. et al., 2019).

PEI is also a common transfectant. PEI is a positively charged cationic polymer that combines with negatively charged miRNA through electrostatic interactions, and it promotes miRNA escape from lysosomes through the "proton sponge" effect to avoid degradation (Carthew et al., 2020; Hosseinpour et al., 2021). However, the cytotoxicity of PEI is its disadvantage. Therefore, constructing low toxicity PEI-based transport materials is a research direction (Bu et al., 2020). Lim et al. constructed ascorbic acid-PEI carbon dots (CDs) by taking advantage of the characteristics of low toxicity, high biocompatibility and chemical inertia of carbon dots, and they reported that the transfection efficiency of miR-2861 into BMSCs was 47.44% (Lim et al., 2015; Bu et al., 2020) (**Figure 6**). Ou et al. constructed a PEI-functionalized graphene oxide (GO) complex to transfect miR-214 inhibitor into mouse osteoblastic cells (MC3T3-E1), which did not show significant cytotoxicity (Ou et al., 2019).

Information on the transfection vectors, including loading mode, and efficiency as well as release mode, miRNA stability, biocompatibility, and cytotoxicity (Arriaga et al., 2019), is summarized in **Table 3**.

In addition, some materials that have not yet been used in bone tissue engineering can deliver miRNA, such as carbon nanotubes. Carbon nanotubes (CNTs) are nanomaterials whose advantages include high surface-to-volume ratios, needle-like structures, high strength, high stability, good biocompatibility, flexible interactions with carrying materials, high drug-loading capacity and ability to release drugs at specific targets. However, the disadvantages include a lack of biodegradability and toxicity (Zare et al., 2021). Andrea et al. used coated low toxicity carbon nanotubes to deliver miR-503 to mouse endothelial cells, which not only improved the stability of miR-503 but also promoted angiogenesis *in vivo* (Masotti et al., 2016). These studies provide ideas for the formation of vascularized bone in bone defects.

3 OTHER TYPES OF METHODS TO TRANSFECT MIRNA INTO CELLS

Exosomes are lipid structural vesicles with a diameter of 50–100 nm formed by stem cells. Exosomes deliver bioactive proteins, lipids, and RNA to target cells for intercellular communication, and they have characteristics of high compatibility, low toxicity, and low immune stimulation (Chiang et al., 2021; Nan et al., 2021). Exosomes secreted by osteoblasts inhibit the differentiation of osteoclast progenitor cells (Wang Q. et al., 2021). Exosomes derived from M2 macrophages (M2D-Exos) inhibit adipogenesis and promote osteogenesis of BMSCs (Li Z. et al., 2021). Therefore, Nan et al. constructed exosomes from miRNA-378-transfected adipose-derived stem cells (ASCs) and cocultured the extracted exosomes with BMSCs and human umbilical vein endothelial cells (HUVECs). The results showed that miR-378-ASCs-Exos promoted the osteogenic differentiation of BMSCs and improved the angiogenesis of HUVECs *in vitro*, and they enhanced neovascularization and osteogenesis *in vivo* in a glucocorticoid (GC)-induced osteonecrosis of the femoral head (ONFH) rat model (Nan et al., 2021). Peng et al. extracted exosomes produced by BMSCs transfected with a miR-196a simulant or inhibitor and cocultured them with HFOB1.19 osteoblasts. The results showed that the BMSC-Exos entered HFOB1.19 cells and that exosomes overexpressing miR-196a promoted osteogenic differentiation and inhibited HFOB1.19 cell apoptosis (Peng et al., 2021). However, at present, the loading and excretion mechanism of exosomes is still unclear, and the cargo is often retained in exosomes (Chiang et al., 2021).

In addition, there are some carrier-free delivery methods. Lee et al. used a microbubble-ultrasound system. These researchers first constructed the femoral fracture in mice, and miR-29b-3p was injected through the tail vein. The probe was then immediately placed on the skin of the fracture site, and the site was irradiated with ultrasound for 4 min, which allowed the miRNA to be delivered to highly vascularized callus (Lee et al., 2016). Tu et al. injected agomiR-142-5p directly at the periosteal of the fracture site once a week for 4 weeks (Tu et al., 2017). Qin et al. isolated an extracellular vesicle (EV) delivery system from BMSCs, and the resulting EVs were rich in miR-196a, miR-27a, and miR-206. The results showed that after the EVs entered osteoblasts through endocytosis, they existed in the endoplasmic reticulum, Golgi apparatus, and lysosomes, releasing cargo along the way (Qin et al., 2016). However, the transfection efficiency and the tissue toxicity of the methods were not shown in the above studies.

4 EVALUATION OF NONVIRAL VECTORS

4.1 The Physicochemical and Biological Properties of Nonviral miRNA-Transfected Biomaterials

Various physicochemical and biological properties of nonviral miRNA-transfected biomaterials deserve attention, which are

necessary to promote osteogenic gene expression and osteogenic differentiation of target cells.

Most studies have reported the zeta potential of carrier materials. Zeta potential is the potential difference between the mobile dispersion medium and the fluid stationary layer attached to the dispersed particles, which can be directly measured by electromotive phenomena (Lu and Gao, 2010). Zeta potential is generally used to evaluate or predict the physical stability of particle dispersion systems (Ding et al., 2018). Generally, the higher the absolute value of zeta potential, the greater the electrostatic repulsion between particles, that is, dissolution or dispersion can resist aggregation, and the better the physical stability (Lu and Gao, 2010). It is generally believed that the zeta potential value of an electrostatically stable suspension should reach at least ±30 mV. On the other hand, low values, less than 5 mV, can cause agglomeration (Gumustas et al., 2017). In the experiment of Professor Liu (Liu et al., 2018b), a multibiological delivery vector was created to encapsulate miR-10a, which contained poly(l-lactic acid) (PLLA)/polyethylene glycol (PEG) co-functionalized mesoporous silica nanoparticles (MSN), and poly(lactic acid-co-glycolic acid) microspheres (PLGA MS). However, the zeta potential of the complex was 12 mV. Pan et al. created a PEI-capped gold nanoparticle to deliver miR-29b, and the zeta potential was +9.34 mV when the optimal w/w ratio between nanoparticles and miR-29b was selected as 3 (Pan et al., 2016). The stability of the above system deserves attention.

In terms of loading modes, nucleic acid materials combine with miRNA mainly through complementary base pairing (Li S. et al., 2021). The combination mode of calcium phosphates is electrostatic interaction (Mencía Castaño et al., 2019). Nanoparticles load miRNA through chemical bond, including coordination bond (Liu et al., 2021) and covalent bond (Abu-Laban et al., 2019), or intermolecular force, including electrostatic interaction (Yang L. et al., 2021), physical adsorption (Yu et al., 2017), or light-activated connection (Qureshi et al., 2013; Moncal et al., 2019). Nanocapsules encapsulate miRNA through electrostatic interaction, hydrogen bonding, or a network polymer formed by free radical polymerization (Liu et al., 2015; Meng et al., 2016b; Geng et al., 2018). Other types of nonviral vehicles bind miRNA mainly by electrostatic interaction, such as ascorbic Acid-PEI Carbon Dots (CD) (Bu et al., 2020), PEI-functionalized graphene oxide (GO) complex (Ou et al., 2019), silk-based orthopedic devices (James et al., 2019), low molecular weight protamine (LMWP) (Suh et al., 2013), and comb-shaped polycation (HA-SS-PGEA) consisting of hyaluronic acid (HA), disulfide groups, and ethanolamine (EA)-functionalized poly(glycidyl methacrylate) (PGMA) (Li et al., 2020).

The way for virus vectors to enter cells is gathering on the cell surface through adhesion factors, and then endocytosis is started by the real signal protein, invasion receptor (Mercer et al., 2020). Similarly, nonviral vectors carrying miRNAs enter cells mainly through endocytosis. Receptor-mediated endocytosis is currently recognized as a main way for organisms to ingest biological macromolecules. Li et al. created a unique tetrahedral DNA framework structure so that it can smoothly pass through cell membranes along caveolin-mediated endocytosis (Li S. et al.,

2021). Another common endocytosis is mediated by clathrin (Bu et al., 2020). It has been reported that the pits of clathrin coating cover 2% of the plasma membrane. Because their life span is about 1 min on average, about 2% of the cell surface membrane is internalized every minute (Donaldson, 2013). It is reported that positively charged nanoparticles are generally considered to be able to electrostatically combine with anionic cell membranes to produce positive endocytosis and improve transfection efficiency (Lei et al., 2019; Yang L. et al., 2021).

For the unloading mode, nucleic acid vectors separated from miRNA by the cut of RNase H (Li S. et al., 2021). Calcium phosphates dissolve in the acidic environment of endocytic vesicles to release miRNA (Mencía Castaño et al., 2019). For nanoparticles, there are many ways to release miRNA. For some cationic nanoparticles, such as PEI nanoparticles, they first efficiently escape from the endosomes mediated by the proton sponge effect into the cytoplasm. PEI contain different types of amino groups, and their pKa values span the physiological pH range, resulting in a buffer capacity. When miR-PEI complexes are encapsulated in the membrane invagination to form endosomes, the environmental pH is in normal physiological range, so the PEI nanoparticles are inactive. However, when the endosomes are combined with lysosomes, the pH value decreases. The unsaturated amino groups on the particles chelate the protons captured by a vacuolar-type H^+-ATPase (V-ATPase) proton pump, which cause lysosomes capturing a large number of protons, and Cl^- and water molecules influx. Cl^- and water molecules cause retention in lysosomes, causing lysosomes swelling and rupture, and the release of particles (Omote and Moriyama, 2013; Bu et al., 2020; Yang L. et al., 2021; Wang et al., 2022). When the complex is released into the cytoplasm, glutathione (GSH) can break down disulfide bonds (Lei et al., 2019), irradiation or discrete photo-trigger can release miRNA from the light-activated link (Qureshi et al., 2013; Moncal et al., 2019), photothermal release at temperature no less than 60°C or the irradiation that is about 400 nm causes the decomposition of covalent bonds (Abu-Laban et al., 2019). For nanocapsules, the acid environment decomposes the electrostatic interactions, hydrogen bonds, and the wrapping of free radical polymerization nets between the carrier material and miRNA (Liu et al., 2015).

In terms of stability, all types of carriers performed well. PBS (Lei et al., 2019), FBS (Yu et al., 2017), serum (Yang L. et al., 2021), heparin (Liu et al., 2015; Meng et al., 2016b), and nuclease (Xue et al., 2017) including RNase A (Li S. et al., 2021)are commonly used materials to detect the ability of the vectors protecting miRNA. Generally, the carriers and miRNA complex is cultured with one of the above materials for 24 h, and then the integrity of miRNA is tested to verify the ability of the vectors to protect miRNA from degradation.

4.2 Comparison of Various Nonviral miRNA-Transfected Biomaterials

For the selection of different types of miRNA vectors, many studies have utilized commercial lipid products because they have

clear transfection effects; therefore, commercial lipid products are often the control group in the research of other miRNA vectors (Carthew et al., 2020). Moreover, commercial lipid products still have low toxicity to cells (Liu Q. et al., 2019).

In contrast, nucleic acid transporters have better biocompatibility. Lipofectamine 2000 was obviously toxic to BMSCs when carrying 500 nm miR, while stFNA changed cell viability only when carrying 4 times the amount of miR carried by Lipofectamine 2000 (Li S. et al., 2021). However, the transfection efficiency of nucleic acid transporters may be lower than that of other types of vectors (Li et al., 2022).

Similarly, The disadvantage of calcium phosphates is that the delivery efficiency is lower than that of Lipofectamine 2000, PEG or PEI, but calcium phosphates are low-toxicity, biodegradable and easy to use (Mencía Castaño et al., 2015).

In addition, nanoparticles and nanocapsules are currently the most studied carriers. Nanomaterials are mostly connected to miRNA through electrostatic interactions. Nanoparticles include inorganic nanoparticles and organic nanoparticles. Inorganic nanoparticles are relatively smaller. For example, the volumes of silica nanoparticles (SNs) and bioactive glass nanoparticles (BGNs) are less than one hundredth of the volume of nanohydroxyapatite (nHA) particles or Lipofectamine RNAi max (Kureel et al., 2017; Yu et al., 2017; Mencía Castaño et al., 2019). However, the release time of organic particles is relatively long, ranging from 100 h to 50 days (Chen X. et al., 2015; Wang et al., 2016; Liu et al., 2018b; Wu et al., 2018; Geng et al., 2020; Jiang et al., 2020). At the same time, nanoparticles well protect miRNA from the degradation of nuclease, serum, and heparin (Meng et al., 2016b; Yan et al., 2020; Yang L. et al., 2021). However, the transfection efficiencies of various types of nanoparticles are quite different, but the efficiencies may also be related to the different types of transfected cells and the different types of miRNA (Liu et al., 2015; Wu G. et al., 2016; Pan et al., 2016; Xue et al., 2017; Yu et al., 2017; Abu-Laban et al., 2019; Liu Q. et al., 2019).

At present, the transfection efficiencies of bioactive glass and Lipofectamine RNAi Max are the highest, more than 90% (Carthew et al., 2020). However, studies have shown that bioactive glass has cytotoxicity. When the concentration of bioactive glass was greater than 100 μg/ml, the cell morphology became irregular, and the live cell attachment was not good with concentrations greater than 240 μg/ml (Li H et al., 2017; Yu et al., 2017).

In addition, the "indirect" transfection method of extracting exosomes from miRNA-transfected cells and coculturing them with target cells seems to reduce cytotoxicity, which is an interesting new idea.

4.3 The Superiority and Insufficiency of Nonviral miRNA-Transfected Biomaterials

The performance of a carrier can be comprehensively evaluated from the aspects of load efficiency, release efficiency, cell uptake rate, biocompatibility, stability, biological immunity, manufacturing difficulty, cost, osteogenesis time, and *in vivo* experimental osteogenic effect. It is certain that the materials

with high loading and unloading efficiency, high transfection efficiency, favorable stability, and low toxicity are the most ideal. These properties will allow miRNA to fully promote bone regeneration.

Compared to viral materials, nonviral materials have unique advantages, including low toxicity, low immunogenicity, good stability, high loading capacity, flexible design, controllable biodegradability, and relatively simple production and construction processes, and they lack the insertion mutation risk brought by viral vectors. In addition, nonviral materials are less likely to cause local acute reactions, thus allowing repeated administrations (Al-Dosari and Gao, 2009). Most importantly, various studies have shown that the application of nonviral miRNA delivery materials stably and efficiently deliver miRNAs, significantly enhancing the expression levels of osteogenic genes in target cells, the activity of osteogenic-related enzymes, the differentiation of stem cells into osteoblasts, and the deposition of calcifications, ultimately promoting osteogenesis. Some miR delivery material complexes also enhance nerve and vascular regeneration to assist bone regeneration.

However, there are still some insufficiency of nonviral miRNA-transfected biomaterials. To date, the transfection efficiency of nonviral biological delivery materials is still generally lower than that of viral vectors (Jiao et al., 2020). The reason may be that the viral vectors have adhesion factors and specific invasion receptors. The former can make the vectors gather on the cell surface, and the latter can promote endocytosis and improve the efficiency of the vectors entering the cell. Hence, it is needy to enhance the surface specificity of nonviral vectors through physical and chemical methods to increase the efficiency of cellular uptake. Second, some materials have slight toxicity to cells, tissues, and organs. It is important to reduce or even eliminate their toxicity and further improve histocompatibility. Third, the types of carriers, the types of miRNA, the types of stem cells, material concentrations, and the animal models used in different experiments are quite different, and the observation time reported in different literatures is also different. Quantitative comparison in the loading efficiency and the cell transfection efficiency between different materials is absent. Only a few experiments use commercial lipofectamine transfectants as the control group for comparison. More experiments that control the variables of miRNA, cell types, and animal models are needed to detect the transfection ability of different transfection materials. Fourth, few literatures report the reason why they chose the certain kind of vector. Different kinds of miRNA and stem cells may have their own suitable transfection materials to meet the best their unique properties, but unfortunately, there is no related discussion in the literatures. Finally, there are still some new and promising biological materials that can deliver miRNA but have not been sufficiently applied to bone tissue engineering, such as carbon nanotubes and exosomes. These new materials can be tested more for their miRNA transfection efficiency and bone regeneration effects *in vivo* and *in vitro* to develop new or compound carriers to improve the safety, efficiency, and targeting of miRNA delivery materials in bone tissue engineering.

5 CONCLUSION

With the development of bone tissue regeneration engineering, researchers have gradually realized that miRNAs play an important role in bone regeneration. Research on miRNA-loaded biomaterials is of great significance in bone tissue regeneration engineering because miRNA delivery materials protect miRNAs from degradation in the release process, extending the release time and making the process more controllable, stable, and efficient. Among existing delivery biomaterials, nonviral miRNA delivery materials are increasingly used in bone tissue regeneration engineering because they overcome the shortcomings of viral materials.

In short, we reviewed the properties of miRNA-transfected materials used in different bone regeneration engineering studies, including calcium phosphates, nanosystems, liposomes, nucleic acids, silk-based biomaterials, cell-penetrating peptides, bioactive glass, and PEI (**Figure 7**).

For the existing defects of nonviral vectors, such as relatively low transfection efficiency and the lack of quantitative comparison, future research should focus on overcoming these problems, developing new or compound carriers, improving the safety, specificity, and the transfection efficiency of the materials through physical or chemical methods, so that miRNA transfection vectors can be better used in bone tissue engineering.

AUTHOR CONTRIBUTIONS

Conceptualization, NZ, XX, and YB; writing—original draft preparation, MZ, and YG; writing—review and editing, YG and CB; supervision, NZ; funding acquisition, NZ.

FUNDING

REFERENCES

Abu-Laban, M., Hamal, P., Arrizabalaga, J. H., Forghani, A., Dikkumbura, A. S., Kumal, R. R., et al. (2019). Combinatorial Delivery of miRNA-Nanoparticle Conjugates in Human Adipose Stem Cells for Amplified Osteogenesis. *Small* 15 (50), 1902864. doi:10.1002/smll.201902864

Akkouch, A., Eliason, S., Sweat, M. E., Romero-Bustillos, M., Zhu, M., Qian, F., et al. (2019). Enhancement of MicroRNA-200c on Osteogenic Differentiation and Bone Regeneration by Targeting Sox2-Mediated Wnt Signaling and Klf4. *Hum. Gene Ther.* 30 (11), 1405–1418. doi:10.1089/hum.2019.019

Al-Dosari, M. S., and Gao, X. (2009). Nonviral Gene Delivery: Principle, Limitations, and Recent Progress. *Aaps J.* 11 (4), 671–681. doi:10.1208/s12248-009-9143-y

Arriaga, M. A., Ding, M. H., Gutierrez, A. S., and Chew, S. A. (2019). The Application of microRNAs in Biomaterial Scaffold-Based Therapies for Bone Tissue Engineering. *Biotechnol. J.* 14 (10), 1900084. doi:10.1002/biot.201900084

Bakan, F. (2018). "Gene Delivery by Hydroxyapatite and Calcium Phosphate Nanoparticles: A Review of Novel and Recent Applications," in *Hydroxyapatite - Advances in Composite Nanomaterials, Biomedical Applications and its Technological Facets*. doi:10.5772/intechopen.71062

Balagangadharan, K., Viji Chandran, S., Arumugam, B., Saravanan, S., Devanand Venkatasubbu, G., and Selvamurugan, N. (2018). Chitosan/nano-hydroxyapatite/nano-zirconium Dioxide Scaffolds with miR-590-5p for Bone Regeneration. *Int. J. Biol. Macromol.* 111, 953–958. doi:10.1016/j.ijbiomac.2018.01.122

Bose, S., and Tarafder, S. (2012). Calcium Phosphate Ceramic Systems in Growth Factor and Drug Delivery for Bone Tissue Engineering: a Review. *Acta Biomater.* 8 (4), 1401–1421. doi:10.1016/j.actbio.2011.11.017

Brenner, T., Posa-Markaryan, K., Posa-Markaryan, K., Hercher, D., Sperger, S., Heimel, P., et al. (2021). Evaluation of BMP2/miRNA Co-Expression Systems for Potent Therapeutic Efficacy in Bone-Tissue Regeneration. *eCM* 41, 245–268. doi:10.22203/eCM.v041a18

Bu, W., Xu, X., Wang, Z., Jin, N., Liu, L., Liu, J., et al. (2020). Ascorbic Acid-PEI Carbon Dots with Osteogenic Effects as miR-2861 Carriers to Effectively Enhance Bone Regeneration. *ACS Appl. Mat. Interfaces* 12 (45), 50287–50302. doi:10.1021/acsami.0c15425

Carter, M., and Shieh, J. (2015). "Gene Delivery Strategies," in *Guide to Research Techniques in Neuroscience*, 239–252. doi:10.1016/b978-0-12-800511-8.00011-3

Carthew, J., Donderwinkel, I., Shrestha, S., Truong, V. X., Forsythe, J. S., and Frith, J. E. (2020). *In Situ* miRNA Delivery from a Hydrogel Promotes Osteogenesis of Encapsulated Mesenchymal Stromal Cells. *Acta Biomater.* 101, 249–261. doi:10.1016/j.actbio.2019.11.016

Castaño, I. M., Raftery, R. M., Chen, G., Cavanagh, B., Quinn, B., Duffy, G. P., et al. (2020). Rapid Bone Repair with the Recruitment Of Cd206 [+] M2-Like Macrophages Using Non-Viral Scaffold-Mediated Mir-133a Inhibition Of Host Cells. *Acta Biomater.* 109, 267–279. doi:10.1016/j.actbio.2020.03.042

Chang, C.-C., Venø, M. T., Chen, L., Ditzel, N., Le, D. Q. S., Dillschneider, P., et al. (2018). Global MicroRNA Profiling in Human Bone Marrow Skeletal-Stromal or Mesenchymal-Stem Cells Identified Candidates for Bone Regeneration. *Mol. Ther.* 26 (2), 593–605. doi:10.1016/j.ymthe.2017.11.018

Chen, X., Gu, S., Chen, B.-F., Shen, W.-L., Yin, Z., Xu, G.-W., et al. (2015). Nanoparticle Delivery of Stable miR-199a-5p Agomir Improves the Osteogenesis of Human Mesenchymal Stem Cells via the HIF1a Pathway. *Biomaterials* 53, 239–250. doi:10.1016/j.biomaterials.2015.02.071

Chen, Y., Gao, D.-Y., and Huang, L. (2015). *In Vivo* delivery of miRNAs for Cancer Therapy: Challenges and Strategies. *Adv. Drug Deliv. Rev.* 81, 128–141. doi:10.1016/j.addr.2014.05.009

Chen, M., Zhou, M., Fu, Y., Li, J., and Wang, Z. (2021). Effects of miR-672 on the Angiogenesis of Adipose-Derived Mesenchymal Stem Cells during Bone Regeneration. *Stem Cell Res. Ther.* 12 (1), 85. doi:10.1186/s13287-021-02154-7

Chiang, C.-L., Cheng, M.-H., and Lin, C.-H. (2021). From Nanoparticles to Cancer Nanomedicine: Old Problems with New Solutions. *Nanomaterials* 11 (7), 1727. doi:10.3390/nano11071727

Curtin, C. M., Tierney, E. G., McSorley, K., Cryan, S.-A., Duffy, G. P., and O'Brien, F. J. (2015). Combinatorial Gene Therapy Accelerates Bone Regeneration: Non-viral Dual Delivery of VEGF and BMP2 in a Collagen-Nanohydroxyapatite Scaffold. *Adv. Healthc. Mat.* 4 (2), 223–227. doi:10.1002/adhm.201400397

Dasari, A., Xue, J., and Deb, S. (2022). Magnetic Nanoparticles in Bone Tissue Engineering. *Nanomaterials* 12 (5), 757. doi:10.3390/nano12050757

Dasgupta, I., and Chatterjee, A. (2021). Recent Advances in miRNA Delivery Systems. *Methods Protoc.* 4 (1), 10. doi:10.3390/mps4010010

Delyagina, E., Li, W., Ma, N., and Steinhoff, G. (2011). Magnetic Targeting Strategies in Gene Delivery. *Nanomedicine* 6 (9), 1593–1604. doi:10.2217/nnm.11.143

Deng, Y., Zhou, H., Zou, D., Xie, Q., Bi, X., Gu, P., et al. (2013). The Role of miR-31-Modified Adipose Tissue-Derived Stem Cells in Repairing Rat Critical-Sized

Calvarial Defects. *Biomaterials* 34 (28), 6717–6728. doi:10.1016/j.biomaterials.2013.05.042

Deng, Y., Bi, X., Bi, X., Zhou, H., You, Z., Wang, Y., et al. (2014). Repair of Critical-Sized Bone Defects with Anti-miR-31-expressing Bone Marrow Stromal Stem Cells and Poly(glycerol Sebacate) Scaffolds. *Eur. Cell Mater* 27, 13–25. doi:10.22203/ecm.v027a02

Ding, Z., Jiang, Y., and Liu, X. (2018). "Nanoemulsions-Based Drug Delivery for Brain Tumors," in *Nanotechnology-Based Targeted Drug Delivery Systems for Brain Tumors*. Editors P. Kesharwani and U. Gupta (Academic Press), 327–358. doi:10.1016/b978-0-12-812218-1.00012-9

Ding, Y., Yin, Y., Hou, Y., Jiang, H., Zhang, J., Dai, Z., et al. (2020). microRNA-214-3p Suppresses Ankylosing Spondylitis Fibroblast Osteogenesis via BMP-Tgfβ Axis and BMP2. *Front. Endocrinol.* 11, 609753. doi:10.3389/fendo.2020.609753

Ding, R., Liu, X., Zhang, J., Yuan, J., Zheng, S., Cheng, X., et al. (2021). Downregulation of miR-1-3p Expression Inhibits the Hypertrophy and Mineralization of Chondrocytes in DDH. *J. Orthop. Surg. Res.* 16 (1), 512. doi:10.1186/s13018-021-02666-1

Donaldson, J. G. (2013). "Endocytosis," in *Encyclopedia of Biological Chemistry*. Editors W. J. Lennarz and M. D. Lane. Second Edition (Waltham: Academic Press), 197–199. doi:10.1016/b978-0-12-378630-2.00121-3

Fang, T., Wu, Q., Zhou, L., Mu, S., and Fu, Q. (2016). miR-106b-5p and miR-17-5p Suppress Osteogenic Differentiation by Targeting Smad5 and Inhibit Bone Formation. *Exp. Cell Res.* 347 (1), 74–82. doi:10.1016/j.yexcr.2016.07.010

Fuerkaiti, S. N., Çakmak, A. S., Karaaslan, C., and Gümüşderelioğlu, M. (2022). Enhanced Osteogenic Effect in Reduced BMP-2 Doses with siNoggin Transfected Pre-osteoblasts in 3D Silk Scaffolds. *Int. J. Pharm.* 612, 121352. doi:10.1016/j.ijpharm.2021.121352

Gan, M., Zhou, Q., Ge, J., Zhao, J., Wang, Y., Yan, Q., et al. (2021). Precise *In-Situ* Release of microRNA from an Injectable Hydrogel Induces Bone Regeneration. *Acta Biomater.* 135, 289–303. doi:10.1016/j.actbio.2021.08.041

Gantenbein, B., Tang, S., Guerrero, J., Higuita-Castro, N., Salazar-Puerta, A. I., Croft, A. S., et al. (2020). Non-viral Gene Delivery Methods for Bone and Joints. *Front. Bioeng. Biotechnol.* 8, 598466. doi:10.3389/fbioe.2020.598466

Geng, Z., Wang, X., Zhao, J., Li, Z., Ma, L., Zhu, S., et al. (2018). The Synergistic Effect of Strontium-Substituted Hydroxyapatite and microRNA-21 on Improving Bone Remodeling and Osseointegration. *Biomater. Sci.* 6 (10), 2694–2703. doi:10.1039/c8bm00716k

Geng, Z., Yu, Y., Li, Z., Ma, L., Zhu, S., Liang, Y., et al. (2020). miR-21 Promotes Osseointegration and Mineralization through Enhancing Both Osteogenic and Osteoclastic Expression. *Mater. Sci. Eng. C* 111, 110785. doi:10.1016/j.msec.2020.110785

Goodwin, T., and Huang, L. (2014). Nonviral Vectors. *Adv. Genet.* 88, 1–12. doi:10.1016/B978-0-12-800148-6.00001-8

Grixti, J. M., Ayers, D., and Day, P. J. R. (2021). An Analysis of Mechanisms for Cellular Uptake of miRNAs to Enhance Drug Delivery and Efficacy in Cancer Chemoresistance. *Noncoding RNA* 7 (2), 27. doi:10.3390/ncrna7020027

Gumustas, M., Sengel-Turk, C. T., Gumustas, A., Ozkan, S. A., and Uslu, B. (2017). "Effect of Polymer-Based Nanoparticles on the Assay of Antimicrobial Drug Delivery Systems," in *Multifunctional Systems for Combined Delivery, Biosensing and Diagnostics*. Editor A. M. Grumezescu (Elsevier), 67–108. doi:10.1016/b978-0-323-52725-5.00005-8

Han, X., Xu, H., Che, L., Sha, D., Huang, C., Meng, T., et al. (2020). RETRACTED: Application of Inorganic Nanocomposite Hydrogels in Bone Tissue Engineering. *iScience* 23 (12), 101845. doi:10.1016/j.isci.2020.101845

Hong, L., Sharp, T., Khorsand, B., Fischer, C., Eliason, S., Salem, A., et al. (2016). MicroRNA-200c Represses IL-6, IL-8, and CCL-5 Expression and Enhances Osteogenic Differentiation. *Plos One* 11 (8), e0160915. doi:10.1371/journal.pone.0160915

Hori, M. (2019). "General Introduction," in *Plasma Medical Science*, 1–4. doi:10.1016/b978-0-12-815004-7.00001-9

Hoseinzadeh, S., Atashi, A., Soleimani, M., Alizadeh, E., and Zarghami, N. (2016). MiR-221-inhibited Adipose Tissue-Derived Mesenchymal Stem Cells Bioengineered in a Nano-Hydroxy Apatite Scaffold. *Vitro Cell.Dev.Biol.-Animal* 52 (4), 479–487. doi:10.1007/s11626-015-9992-x

Hosseinpour, S., Cao, Y., Liu, J., Xu, C., and Walsh, L. J. (2021). Efficient Transfection and Long-Term Stability of Rno-miRNA-26a-5p for Osteogenic Differentiation by Large Pore Sized Mesoporous Silica Nanoparticles. *J. Mat. Chem. B* 9 (9), 2275–2284. doi:10.1039/d0tb02756a

Hou, Y., Lin, W., Li, Y., Sun, Y., Liu, Y., Chen, C., et al. (2021). De-osteogenic-differentiated Mesenchymal Stem Cells Accelerate Fracture Healing by Mir-92b. *J. Orthop. Transl.* 27, 25–32. doi:10.1016/j.jot.2020.10.009

Huynh, C. T., Nguyen, M. K., Naris, M., Tonga, G. Y., Rotello, V. M., and Alsberg, E. (2016). Light-triggered RNA Release and Induction of hMSC Osteogenesis via Photodegradable, Dual-Crosslinked Hydrogels. *Nanomedicine* 11 (12), 1535–1550. doi:10.2217/nnm-2016-0088

Iaquinta, M. R., Mazzoni, E., Bononi, I., Rotondo, J. C., Mazziotta, C., Montesi, M., et al. (2019). Adult Stem Cells for Bone Regeneration and Repair. *Front. Cell Dev. Biol.* 7, 268. doi:10.3389/fcell.2019.00268

James, E. N., Delany, A. M., and Nair, L. S. (2014). Post-Transcriptional Regulation in Osteoblasts Using Localized Delivery of miR-29a Inhibitor from Nanofibers to Enhance Extracellular Matrix Deposition. *Acta Biomater.* 10 (8), 3571–3580. doi:10.1016/j.actbio.2014.04.026

James, E. N., Van Doren, E., Li, C., and Kaplan, D. L. (2019). Silk Biomaterials-Mediated miRNA Functionalized Orthopedic Devices. *Tissue Eng. Part A* 25 (1-2), 12–23. doi:10.1089/ten.TEA.2017.0455

Jiang, F., Yin, F., Lin, Y., Xia, W., Zhou, L., Pan, C., et al. (2020). The Promotion of Bone Regeneration through CS/GP-CTH/antagomir-133a/b Sustained Release System. *Nanomedicine Nanotechnol. Biol. Med.* 24, 102116. doi:10.1016/j.nano.2019.102116

Jiang, W., Zhu, P., Zhang, T., Liao, F., Yu, Y., Liu, Y., et al. (2021). MicroRNA-205 Mediates Endothelial Progenitor Functions in Distraction Osteogenesis by Targeting the Transcription Regulator NOTCH2. *Stem Cell Res. Ther.* 12 (1), 101. doi:10.1186/s13287-021-02150-x

Jiao, Y., Xia, Z. L., Ze, L. J., Jing, H., Xin, B., and Fu, S. (2020). Research Progress of Nucleic Acid Delivery Vectors for Gene Therapy. *Biomed. Microdevices* 22 (1), 16. doi:10.1007/s10544-020-0469-7

Kang, M., Lee, C.-S., and Lee, M. (2021). Bioactive Scaffolds Integrated with Liposomal or Extracellular Vesicles for Bone Regeneration. *Bioengineering* 8 (10), 137. doi:10.3390/bioengineering8100137

Kashapov, R., Ibragimova, A., Pavlov, R., Gabdrakhmanov, D., Kashapova, N., Burilova, E., et al. (2021). Nanocarriers for Biomedicine: From Lipid Formulations to Inorganic and Hybrid Nanoparticles. *Int. J. Mol. Sci.* 22 (13), 7055. doi:10.3390/ijms22137055

Kureel, J., John, A. A., Dixit, M., and Singh, D. (2017). MicroRNA-467g Inhibits New Bone Regeneration by Targeting Ihh/Runx-2 Signaling. *Int. J. Biochem. Cell Biol.* 85, 35–43. doi:10.1016/j.biocel.2017.01.018

Lanzillotti, C., De Mattei, M., Mazziotta, C., Taraballi, F., Rotondo, J. C., Tognon, M., et al. (2021). Long Non-coding RNAs and MicroRNAs Interplay in Osteogenic Differentiation of Mesenchymal Stem Cells. *Front. Cell Dev. Biol.* 9, 646032. doi:10.3389/fcell.2021.646032

Lee, W. Y., Li, N., Lin, S., Wang, B., Lan, H. Y., and Li, G. (2016). miRNA-29b Improves Bone Healing in Mouse Fracture Model. *Mol. Cell. Endocrinol.* 430, 97–107. doi:10.1016/j.mce.2016.04.014

Lei, L., Liu, Z., Yuan, P., Jin, R., Wang, X., Jiang, T., et al. (2019). Injectable Colloidal Hydrogel with Mesoporous Silica Nanoparticles for Sustained Co-release of microRNA-222 and Aspirin to Achieve Innervated Bone Regeneration in Rat Mandibular Defects. *J. Mat. Chem. B* 7 (16), 2722–2735. doi:10.1039/c9tb00025a

Levingstone, T. J., Herbaj, S., Redmond, J., McCarthy, H. O., and Dunne, N. J. (2020). Calcium Phosphate Nanoparticles-Based Systems for RNAi Delivery: Applications in Bone Tissue Regeneration. *Nanomaterials* 10 (1), 146. doi:10.3390/nano10010146

Li, Y., Fan, L., Liu, S., Liu, W., Zhang, H., Zhou, T., et al. (2013). The Promotion of Bone Regeneration through Positive Regulation of Angiogenic-Osteogenic Coupling Using microRNA-26a. *Biomaterials* 34 (21), 5048–5058. doi:10.1016/j.biomaterials.2013.03.052

Li, H., Liu, P., Xu, S., Li, Y., Dekker, J. D., Li, B., et al. (2017). FOXP1 Controls Mesenchymal Stem Cell Commitment and Senescence during Skeletal Aging. *J. Clin. Invest* 127 (4), 1241–1253. doi:10.1172/jci89511

Li, K.-C., Lo, S.-C., Sung, L.-Y., Liao, Y.-H., Chang, Y.-H., and Hu, Y.-C. (2017). Improved Calvarial Bone Repair by hASCs Engineered with Cre/loxP-Based Baculovirus Conferring Prolonged BMP-2 and MiR-148b Co-expression. *J. Tissue Eng. Regen. Med.* 11 (11), 3068–3077. doi:10.1002/term.2208

Li, X., Liang, Q., Zhang, W., Li, Y., Ye, J., Zhao, F., et al. (2017). Bio-inspired Bioactive Glasses for Efficient microRNA and Drug Delivery. *J. Mat. Chem. B* 5 (31), 6376–6384. doi:10.1039/c7tb01021d

Li, R., Wang, H., John, J. V., Song, H., Teusink, M. J., and Xie, J. (2020). 3D Hybrid Nanofiber Aerogels Combining with Nanoparticles Made of a Biocleavable and Targeting Polycation and MiR-26a for Bone Repair. *Adv. Funct. Mat.* 30 (49), 2005531. doi:10.1002/adfm.202005531

Li, S., Liu, Y., Tian, T., Zhang, T., Lin, S., Zhou, M., et al. (2021). Bioswitchable Delivery of microRNA by Framework Nucleic Acids: Application to Bone Regeneration. *Small* 17 (47), 2104359. doi:10.1002/smll.202104359

Li, Z., Wang, Y., Li, S., and Li, Y. (2021). Exosomes Derived from M2 Macrophages Facilitate Osteogenesis and Reduce Adipogenesis of BMSCs. *Front. Endocrinol.* 12, 680328. doi:10.3389/fendo.2021.680328

Li, D., Yang, Z., Luo, Y., Zhao, X., Tian, M., and Kang, P. (2022). Delivery of MiR335-5p-Pendant Tetrahedron DNA Nanostructures Using an Injectable Heparin Lithium Hydrogel for Challenging Bone Defects in Steroid-Associated Osteonecrosis. *Adv. Healthc. Mater.* 11 (1), 2101412. doi:10.1002/adhm.202101412

Liao, Y.-H., Chang, Y.-H., Sung, L.-Y., Li, K.-C., Yeh, C.-L., Yen, T.-C., et al. (2014). Osteogenic Differentiation of Adipose-Derived Stem Cells and Calvarial Defect Repair Using Baculovirus-Mediated Co-expression of BMP-2 and miR-148b. *Biomaterials* 35 (18), 4901–4910. doi:10.1016/j.biomaterials.2014.02.055

Lim, S. Y., Shen, W., and Gao, Z. (2015). Carbon Quantum Dots and Their Applications. *Chem. Soc. Rev.* 44 (1), 362–381. doi:10.1039/c4cs00269e

Liu, N., and Sun, Y. (2021). microRNA-148a-3p-targeting P300 Protects against Osteoblast Differentiation and Osteoporotic Bone Reconstruction. *Regen. Med.* 16 (5), 435–449. doi:10.2217/rme-2020-0006

Liu, C., Wen, J., Meng, Y., Zhang, K., Zhu, J., Ren, Y., et al. (2015). Efficient Delivery of Therapeutic miRNA Nanocapsules for Tumor Suppression. *Adv. Mat.* 27 (2), 292–297. doi:10.1002/adma.201403387

Liu, J., Meng, T., Ming, Y., Wen, L., Cheng, B., Liu, N., et al. (2016). MicroRNA-200c Delivered by Solid Lipid Nanoparticles Enhances the Effect of Paclitaxel on Breast Cancer Stem Cell. *Int. J. Nanomedicine* Vol. 11, 6713–6725. doi:10.2147/ijn.S111647

Liu, Z., Chang, H., Hou, Y., Wang, Y., Zhou, Z., Wang, M., et al. (2018a). Lentivirus-mediated microRNA-26a Overexpression in Bone Mesenchymal Stem Cells Facilitates Bone Regeneration in Bone Defects of Calvaria in Mice. *Mol. Med. Rep.* 18 (6), 5317–5326. doi:10.3892/mmr.2018.9596

Liu, Z., Chen, X., Zhang, Z., Zhang, X., Saunders, L., Zhou, Y., et al. (2018b). Nanofibrous Spongy Microspheres to Distinctly Release miRNA and Growth Factors to Enrich Regulatory T Cells and Rescue Periodontal Bone Loss. *ACS Nano* 12 (10), 9785–9799. doi:10.1021/acsnano.7b08976

Liu, H., Dong, Y., Feng, X., Li, L., Jiao, Y., Bai, S., et al. (2019). miR-34a Promotes Bone Regeneration in Irradiated Bone Defects by Enhancing Osteoblastic Differentiation of Mesenchymal Stromal Cells in Rats. *Stem Cell Res. Ther.* 10 (1), 180. doi:10.1186/s13287-019-1285-y

Liu, J., Dang, L., Wu, X., Li, D., Ren, Q., Lu, A., et al. (2019). microRNA-Mediated Regulation of Bone Remodeling: A Brief Review. *JBMR Plus* 3 (9), e10213. doi:10.1002/jbm4.10213

Liu, Q., Lin, Z., Liu, Y., Du, J., Lin, H., and Wang, J. (2019). Delivery of miRNA-29b Using R9-LK15, a Novel Cell-Penetrating Peptide, Promotes Osteogenic Differentiation of Bone Mesenchymal Stem Cells. *BioMed Res. Int.* 2019, 12. doi:10.1155/2019/3032158

Liu, J., Cui, Y., Kuang, Y., Xu, S., Lu, Q., Diao, J., et al. (2021). Hierarchically Porous Calcium-Silicon Nanosphere-Enabled Co-delivery of microRNA-210 and Simvastatin for Bone Regeneration. *J. Mat. Chem. B* 9 (16), 3573–3583. doi:10.1039/d1tb00063b

Lu, G. W., and Gao, P. (2010). "Emulsions and Microemulsions for Topical and Transdermal Drug Delivery," in *Handbook of Non-invasive Drug Delivery Systems*. Editor V. S. Kulkarni (Boston: William Andrew Publishing), 59–94. doi:10.1016/b978-0-8155-2025-2.10003-4

Marew, T., and Birhanu, G. (2021). Three Dimensional Printed Nanostructure Biomaterials for Bone Tissue Engineering. *Regen. Ther.* 18, 102–111. doi:10.1016/j.reth.2021.05.001

Masotti, A., Miller, M. R., Celluzzi, A., Rose, L., Micciulla, F., Hadoke, P. W. F., et al. (2016). Regulation of Angiogenesis through the Efficient Delivery of microRNAs into Endothelial Cells Using Polyamine-Coated Carbon Nanotubes. *Nanomedicine Nanotechnol. Biol. Med.* 12 (6), 1511–1522. doi:10.1016/j.nano.2016.02.017

Mazziotta, C., Lanzillotti, C., Iaquinta, M. R., Taraballi, F., Torreggiani, E., Rotondo, J. C., et al. (2021). MicroRNAs Modulate Signaling Pathways in Osteogenic Differentiation of Mesenchymal Stem Cells. *Int. J. Mol. Sci.* 22 (5), 2362. doi:10.3390/ijms22052362

McCully, M., Conde, J., Baptista, P., Dalby, M. J., and Berry, C. C. (2018). Nanoparticle-antagomiR Based Targeting of miR-31 to Induce Osterix and Osteocalcin Expression in Mesenchymal Stem Cells. *Plos One* 13 (2), e0192562. doi:10.1371/journal.pone.0192562

Md, S., Alhakamy, N. A., Karim, S., Gabr, G. A., Iqubal, M. K., and Murshid, S. S. A. (2021). Signaling Pathway Inhibitors, miRNA, and Nanocarrier-Based Pharmacotherapeutics for the Treatment of Lung Cancer: A Review. *Pharmaceutics* 13 (12), 2120. doi:10.3390/pharmaceutics13122120

Meech, R., Edelman, D. B., Jones, F. S., and Makarenkova, H. P. (2005). The Homeobox Transcription Factor Barx2 Regulates Chondrogenesis during Limb Development. *Development* 132 (9), 2135–2146. doi:10.1242/dev.01811

Mencía Castaño, I., Curtin, C. M., Duffy, G. P., and O'Brien, F. J. (2016). Next Generation Bone Tissue Engineering: Non-viral miR-133a Inhibition Using Collagen-Nanohydroxyapatite Scaffolds Rapidly Enhances Osteogenesis. *Sci. Rep.* 6, 27941. doi:10.1038/srep27941

Mencía Castaño, I., Curtin, C. M., Duffy, G. P., and O'Brien, F. J. (2019). Harnessing an Inhibitory Role of miR-16 in Osteogenesis by Human Mesenchymal Stem Cells for Advanced Scaffold-Based Bone Tissue Engineering. *Tissue Eng. Part A* 25 (1-2), 24–33. doi:10.1089/ten.TEA.2017.0460

Mencía Castaño, I., Curtin, C. M., Shaw, G., Mary Murphy, J., Duffy, G. P., and O'Brien, F. J. (2015). A Novel Collagen-Nanohydroxyapatite microRNA-Activated Scaffold for Tissue Engineering Applications Capable of Efficient Delivery of Both miR-Mimics and antagomiRs to Human Mesenchymal Stem Cells. *J. Control. Release* 200, 42–51. doi:10.1016/j.jconrel.2014.12.034

Meng, Y.-B., Li, X., Li, Z.-Y., Zhao, J., Yuan, X.-B., Ren, Y., et al. (2015). microRNA-21 Promotes Osteogenic Differentiation of Mesenchymal Stem Cells by the PI3K/β-Catenin Pathway. *J. Orthop. Res.* 33 (7), 957–964. doi:10.1002/jor.22884

Meng, Y., Li, X., Li, Z., Liu, C., Zhao, J., Wang, J., et al. (2016a). Surface Functionalization of Titanium Alloy with miR-29b Nanocapsules to Enhance Bone Regeneration. *ACS Appl. Mat. Interfaces* 8 (9), 5783–5793. doi:10.1021/acsami.5b10650

Meng, Y., Liu, C., Zhao, J., Li, X., Li, Z., Wang, J., et al. (2016b). An Injectable miRNA-Activated Matrix for Effective Bone Regeneration *In Vivo*. *J. Mat. Chem. B* 4 (43), 6942–6954. doi:10.1039/c6tb01790h

Mercer, J., Lee, J. E., Saphire, E. O., and Freeman, S. A. (2020). SnapShot: Enveloped Virus Entry. *Cell* 182 (3), 786. e781. doi:10.1016/j.cell.2020.06.033

Mishra, B., and Singh, J. (2020). "Novel Drug Delivery Systems and Significance in Respiratory Diseases," in *Targeting Chronic Inflammatory Lung Diseases Using Advanced Drug Delivery Systems*, 57–95. doi:10.1016/b978-0-12-820658-4.00004-2

Moncal, K. K., Aydin, R. S. T., Abu-Laban, M., Heo, D. N., Rizk, E., Tucker, S. M., et al. (2019). Collagen-infilled 3D Printed Scaffolds Loaded with miR-148b-Transfected Bone Marrow Stem Cells Improve Calvarial Bone Regeneration in Rats. *Mater. Sci. Eng. C* 105, 110128. doi:10.1016/j.msec.2019.110128

Nan, K., Zhang, Y., Zhang, X., Li, D., Zhao, Y., Jing, Z., et al. (2021). Exosomes from miRNA-378-Modified Adipose-Derived Stem Cells Prevent Glucocorticoid-Induced Osteonecrosis of the Femoral Head by Enhancing Angiogenesis and Osteogenesis via Targeting miR-378 Negatively Regulated Suppressor of Fused (Sufu). *Stem Cell Res. Ther.* 12 (1), 331. doi:10.1186/s13287-021-02390-x

Nayerossadat, N., Ali, P., and Maedeh, T. (2012). Viral and Nonviral Delivery Systems for Gene Delivery. *Adv. Biomed. Res.* 1, 27. doi:10.4103/2277-9175.98152

Nguyen, M. K., Jeon, O., Krebs, M. D., Schapira, D., and Alsberg, E. (2014). Sustained Localized Presentation of RNA Interfering Molecules from *In Situ* Forming Hydrogels to Guide Stem Cell Osteogenic Differentiation. *Biomaterials* 35 (24), 6278–6286. doi:10.1016/j.biomaterials.2014.04.048

Nguyen, M. K., Jeon, O., Dang, P. N., Huynh, C. T., Varghai, D., Riazi, H., et al. (2018). RNA Interfering Molecule Delivery from *In Situ* Forming Biodegradable Hydrogels for Enhancement of Bone Formation in Rat Calvarial Bone Defects. *Acta Biomater.* 75, 105–114. doi:10.1016/j.actbio.2018.06.007

Omote, H., and Moriyama, Y. (2013). Vesicular Neurotransmitter Transporters: an Approach for Studying Transporters with Purified Proteins. *Physiology* 28 (1), 39–50. doi:10.1152/physiol.00033.2012

Ou, L., Lan, Y., Feng, Z., Feng, L., Yang, J., Liu, Y., et al. (2019). Functionalization of SF/HAP Scaffold with GO-PEI-miRNA Inhibitor Complexes to Enhance Bone Regeneration through Activating Transcription Factor 4. *Theranostics* 9 (15), 4525–4541. doi:10.7150/thno.34676

Pan, T., Song, W., Gao, H., Li, T., Cao, X., Zhong, S., et al. (2016). miR-29b-Loaded Gold Nanoparticles Targeting to the Endoplasmic Reticulum for Synergistic Promotion of Osteogenic Differentiation. *ACS Appl. Mat. Interfaces* 8 (30), 19217–19227. doi:10.1021/acsami.6b02969

Peng, H., Lu, S. L., Bai, Y., Fang, X., Huang, H., and Zhuang, X. Q. (2018). MiR-133a Inhibits Fracture Healing via Targeting RUNX2/BMP2. *Eur. Rev. Med. Pharmacol. Sci.* 22 (9), 2519–2526. doi:10.26355/eurrev_201805_14914

Peng, Z., Lu, S., Lou, Z., Li, Z., Li, S., Yang, K., et al. (2021). Exosomes from Bone Marrow Mesenchymal Stem Cells Promoted Osteogenic Differentiation by Delivering miR-196a that Targeted Dickkopf-1 to Activate Wnt/β-Catenin Pathway. *Bioengineered* Epub ahead of print. doi:10.1080/21655979.2021.1996015

Qadir, A. S., Lee, J., Lee, Y. S., Woo, K. M., Ryoo, H. M., and Baek, J. H. (2018). Distal-less Homeobox 3, a Negative Regulator of Myogenesis, Is Downregulated by microRNA-133. *J. Cell Biochem.* 120, 2226–2235. doi:10.1002/jcb.27533

Qin, Y., Wang, L., Gao, Z., Chen, G., and Zhang, C. (2016). Bone Marrow Stromal/ stem Cell-Derived Extracellular Vesicles Regulate Osteoblast Activity and Differentiation *In Vitro* and Promote Bone Regeneration *In Vivo*. *Sci. Rep.* 6, 21961. doi:10.1038/srep21961

Qu, H., Fu, H., Han, Z., and Sun, Y. (2019). Biomaterials for Bone Tissue Engineering Scaffolds: a Review. *RSC Adv.* 9 (45), 26252–26262. doi:10.1039/c9ra05214c

Qureshi, A. T., Monroe, W. T., Dasa, V., Gimble, J. M., and Hayes, D. J. (2013). miR-148b-nanoparticle Conjugates for Light Mediated Osteogenesis of Human Adipose Stromal/stem Cells. *Biomaterials* 34 (31), 7799–7810. doi:10.1016/j.biomaterials.2013.07.004

Rahim, M., Rizvi, S. M. D., Iram, S., Khan, S., Bagga, P. S., and Khan, M. S. (2018). "Interaction of Green Nanoparticles with Cells and Organs," in *Inorganic Frameworks as Smart Nanomedicines*, 185–237. doi:10.1016/b978-0-12-813661-4.00005-5

Raj Preeth, D., Saravanan, S., Shairam, M., Selvakumar, N., Selestin Raja, I., Dhanasekaran, A., et al. (2021). Bioactive Zinc(II) Complex Incorporated PCL/gelatin Electrospun Nanofiber Enhanced Bone Tissue Regeneration. *Eur. J. Pharm. Sci.* 160, 105768. doi:10.1016/j.ejps.2021.105768

Reda El Sayed, S., Cristante, J., Guyon, L., Denis, J., Chabre, O., and Cherradi, N. (2021). MicroRNA Therapeutics in Cancer: Current Advances and Challenges. *Cancers* 13 (11), 2680. doi:10.3390/cancers13112680

Remy, M. T., Akkouch, A., He, L., Eliason, S., Sweat, M. E., Krongbaramee, T., et al. (2021). Rat Calvarial Bone Regeneration by 3D-Printed β-Tricalcium Phosphate Incorporating MicroRNA-200c. *ACS Biomater. Sci. Eng.* 7 (9), 4521–4534. doi:10.1021/acsbiomaterials.0c01756

Rossi, M., Pitari, M. R., Amodio, N., Di Martino, M. T., Conforti, F., Leone, E., et al. (2013). miR-29b Negatively Regulates Human Osteoclastic Cell Differentiation and Function: Implications for the Treatment of Multiple Myeloma-Related Bone Disease. *J. Cell. Physiol.* 228 (7), 1506–1515. doi:10.1002/jcp.24306

Ruedel, A., and Bosserhoff, A. K. (2012). "Transfection Methods," in *Laboratory Methods in Cell Biology*, 163–182. doi:10.1016/b978-0-12-405914-6.00008-1

Samorezov, J. E., and Alsberg, E. (2015). Spatial Regulation of Controlled Bioactive Factor Delivery for Bone Tissue Engineering. *Adv. Drug Deliv. Rev.* 84, 45–67. doi:10.1016/j.addr.2014.11.018

Schade, A., Müller, P., Delyagina, E., Voronina, N., Skorska, A., Lux, C., et al. (2014). Magnetic Nanoparticle Based Nonviral MicroRNA Delivery into Freshly Isolated CD105(+) hMSCs. *Stem Cells Int.* 2014, 11. doi:10.1155/2014/197154

Scheideler, M., Vidakovic, I., and Prassl, R. (2020). Lipid Nanocarriers for microRNA Delivery. *Chem. Phys. Lipids* 226, 104837. doi:10.1016/j.chemphyslip.2019.104837

Shen, W., Sun, B., Zhou, C., Ming, W., Zhang, S., and Wu, X. (2020). CircFOXP1/ FOXP1 Promotes Osteogenic Differentiation in Adipose-derived Mesenchymal Stem Cells and Bone Regeneration in Osteoporosis via miR-33a-5p. *J. Cell. Mol. Med.* 24 (21), 12513–12524. doi:10.1111/jcmm.15792

Sriram, M., Sainitya, R., Kalyanaraman, V., Dhivya, S., and Selvamurugan, N. (2015). Biomaterials Mediated microRNA Delivery for Bone Tissue Engineering. *Int. J. Biol. Macromol.* 74, 404–412. doi:10.1016/j.ijbiomac.2014.12.034

Su, X., Liao, L., Shuai, Y., Jing, H., Liu, S., Zhou, H., et al. (2015). MiR-26a Functions Oppositely in Osteogenic Differentiation of BMSCs and ADSCs Depending on Distinct Activation and Roles of Wnt and BMP Signaling Pathway. *Cell Death Dis.* 6 (8), e1851. doi:10.1038/cddis.2015.221

Suh, J. S., Lee, J. Y., Choi, Y. S., Chong, P. C., and Park, Y. J. (2013). Peptide-mediated Intracellular Delivery of miRNA-29b for Osteogenic Stem Cell Differentiation. *Biomaterials* 34 (17), 4347–4359. doi:10.1016/j.biomaterials.2013.02.039

Sui, L., Wang, M., Han, Q., Yu, L., Zhang, L., Zheng, L., et al. (2018). A Novel Lipidoid-MicroRNA Formulation Promotes Calvarial Bone Regeneration. *Biomaterials* 177, 88–97. doi:10.1016/j.biomaterials.2018.05.038

Sun, M. H., Wang, W. J., Li, Q., Yuan, T., and Weng, W. J. (2018). Autologous Oxygen Release Nano Bionic Scaffold Composite miR-106a Induced BMSCs Enhances Osteoblast Conversion and Promotes Bone Repair through Regulating BMP-2. *Eur. Rev. Med. Pharmacol. Sci.* 22 (21), 7148–7155. doi:10.26355/eurrev_201811_16246

Sun, X., Li, X., Qi, H., Hou, X., Zhao, J., Yuan, X., et al. (2020). MiR-21 Nanocapsules Promote Early Bone Repair of Osteoporotic Fractures by Stimulating the Osteogenic Differentiation of Bone Marrow Mesenchymal Stem Cells. *J. Orthop. Transl.* 24, 76–87. doi:10.1016/j.jot.2020.04.007

Tahmasebi, A., Enderami, S. E., Saburi, E., Islami, M., Yaslianifard, S., Mahabadi, J. A., et al. (2020). Micro-RNA-incorporated Electrospun Nanofibers Improve Osteogenic Differentiation of Human-induced Pluripotent Stem Cells. *J. Biomed. Mater. Res.* 108 (2), 377–386. doi:10.1002/jbm.a.36824

Tarach, P., and Janaszewska, A. (2021). Recent Advances in Preclinical Research Using PAMAM Dendrimers for Cancer Gene Therapy. *Int. J. Mol. Sci.* 22 (6), 2912. doi:10.3390/ijms22062912

Tian, T., Xiao, D., Zhang, T., Li, Y., Shi, S., Zhong, W., et al. (2020). A Framework Nucleic Acid Based Robotic Nanobee for Active Targeting Therapy. *Adv. Funct. Mat.* 31 (5), 2007342. doi:10.1002/adfm.202007342

Tu, M., Tang, J., He, H., Cheng, P., and Chen, C. (2017). MiR-142-5p Promotes Bone Repair by Maintaining Osteoblast Activity. *J. Bone Min. Metab.* 35 (3), 255–264. doi:10.1007/s00774-016-0757-8

Vimalraj, S., Saravanan, S., Vairamani, M., Gopalakrishnan, C., Sastry, T. P., and Selvamurugan, N. (2016). A Combinatorial Effect of Carboxymethyl Cellulose Based Scaffold and microRNA-15b on Osteoblast Differentiation. *Int. J. Biol. Macromol.* 93 (Pt B), 1457–1464. doi:10.1016/j.ijbiomac.2015.12.083

Vishal, M., Vimalraj, S., Ajeetha, R., Gokulnath, M., Keerthana, R., He, Z., et al. (2017). MicroRNA-590-5p Stabilizes Runx2 by Targeting Smad7 During Osteoblast Differentiation. *J. Cell. Physiol.* 232 (2), 371–380. doi:10.1002/jcp.25434

Wang, W., and Yeung, K. W. K. (2017). Bone Grafts and Biomaterials Substitutes for Bone Defect Repair: A Review. *Bioact. Mater.* 2 (4), 224–247. doi:10.1016/j.bioactmat.2017.05.007

Wang, X., Guo, B., Li, Q., Peng, J., Yang, Z., Wang, A., et al. (2013). miR-214 Targets ATF4 to Inhibit Bone Formation. *Nat. Med.* 19 (1), 93–100. doi:10.1038/nm.3026

Wang, Z., Wu, G., Wei, M., Liu, Q., Zhou, J., et al. (2016). Improving the Osteogenesis of Human Bone Marrow Mesenchymal Stem Cell Sheets by microRNA-21-Loaded Chitosan/hyaluronic Acid Nanoparticles via Reverse Transfection. *Int. J. Nanomedicine* 11, 2091–2105. doi:10.2147/ijn.S104851

Wang, Q., Shen, X., Chen, Y., Chen, J., and Li, Y. (2021). Osteoblasts-derived Exosomes Regulate Osteoclast Differentiation through miR-503-3p/Hpse axis. *Acta Histochem.* 123 (7), 151790. doi:10.1016/j.acthis.2021.151790

Wang, Y., He, R., Yang, A., Guo, R., Liu, J., Liang, G., et al. (2021). Role of miR-214 in Biomaterial Transplantation Therapy for Osteonecrosis. *Bme*, 1–14. doi:10.3233/bme-211296

Wang, Q.-y., Yali-Xiang, X., Hu, Q.-h., Huang, S.-h., Lin, J., and Zhou, Q.-h. (2022). Surface Charge Switchable Nano-Micelle for pH/redox-Triggered and Endosomal Escape Mediated Co-delivery of Doxorubicin and Paclitaxel in Treatment of Lung Adenocarcinoma. *Colloids Surfaces B Biointerfaces* 216, 112588. doi:10.1016/j.colsurfb.2022.112588

Wei, J., Li, H., Wang, S., Li, T., Fan, J., Liang, X., et al. (2014). let-7Enhances Osteogenesis and Bone Formation While Repressing Adipogenesis of Human Stromal/Mesenchymal Stem Cells by Regulating HMGA2. *Stem Cells Dev.* 23 (13), 1452–1463. doi:10.1089/scd.2013.0600

Wu, G., Feng, C., Hui, G., Wang, Z., Tan, J., Luo, L., et al. (2016). Improving the Osteogenesis of Rat Mesenchymal Stem Cells by Chitosan-Based-microRNA Nanoparticles. *Carbohydr. Polym.* 138, 49–58. doi:10.1016/j.carbpol.2015.11.044

Wu, S., Liu, W., and Zhou, L. (2016). MiR-590-3p Regulates Osteogenic Differentiation of Human Mesenchymal Stem Cells by Regulating APC Gene. *Biochem. Biophysical Res. Commun.* 478 (4), 1582–1587. doi:10.1016/j.bbrc.2016.08.160

Wu, G., Feng, C., Quan, J., Wang, Z., Wei, W., Zang, S., et al. (2018). *In Situ* controlled Release of Stromal Cell-Derived Factor-1α and antimiR-138 for On-Demand Cranial Bone Regeneration. *Carbohydr. Polym.* 182, 215–224. doi:10.1016/j.carbpol.2017.10.090

Xie, Q., Wang, Z., Zhou, H., Yu, Z., Huang, Y., Sun, H., et al. (2016). The Role of miR-135-Modified Adipose-Derived Mesenchymal Stem Cells in Bone Regeneration. *Biomaterials* 75, 279–294. doi:10.1016/j.biomaterials.2015.10.042

Xie, Q., Wei, W., Ruan, J., Ding, Y., Zhuang, A., Bi, X., et al. (2017). Effects of miR-146a on the Osteogenesis of Adipose-Derived Mesenchymal Stem Cells and Bone Regeneration. *Sci. Rep.* 7, 42840. doi:10.1038/srep42840

Xiong, A., He, Y., Gao, L., Li, G., Weng, J., Kang, B., et al. (2020). Smurf1-targeting miR-19b-3p-Modified BMSCs Combined PLLA Composite Scaffold to Enhance Osteogenic Activity and Treat Critical-Sized Bone Defects. *Biomater. Sci.* 8 (21), 6069–6081. doi:10.1039/d0bm01251c

Xu, G., Ding, Z., and Shi, H.-f. (2019). The Mechanism of miR-889 Regulates Osteogenesis in Human Bone Marrow Mesenchymal Stem Cells. *J. Orthop. Surg. Res.* 14 (1), 366. doi:10.1186/s13018-019-1399-z

Xue, Y., Guo, Y., Yu, M., Wang, M., Ma, P. X., and Lei, B. (2017). Monodispersed Bioactive Glass Nanoclusters with Ultralarge Pores and Intrinsic Exceptionally High miRNA Loading for Efficiently Enhancing Bone Regeneration. *Adv. Healthc. Mat.* 6 (20), 1700630. doi:10.1002/adhm.201700630

Yan, S. G., Zhang, J., Tu, Q. S., Ye, J. H., Luo, E., Schuler, M., et al. (2011). Enhanced Osseointegration of Titanium Implant through the Local Delivery of Transcription Factor SATB2. *Biomaterials* 32 (33), 8676–8683. doi:10.1016/j.biomaterials.2011.07.072

Yan, J., Zhang, C., Zhao, Y., Cao, C., Wu, K., Zhao, L., et al. (2014). Non-viral Oligonucleotide antimiR-138 Delivery to Mesenchymal Stem Cell Sheets and the Effect on Osteogenesis. *Biomaterials* 35 (27), 7734–7749. doi:10.1016/j.biomaterials.2014.05.089

Yan, J., Lu, X., Zhu, X., Hu, X., Wang, L., Qian, J., et al. (2020). Effects of miR-26a on Osteogenic Differentiation of Bone Marrow Mesenchymal Stem Cells by a Mesoporous Silica Nanoparticle - PEI - Peptide System. *Int. J. Nanomedicine* 15, 497–511. doi:10.2147/ijn.S228797

Yang, C., Liu, X., Zhao, K., Zhu, Y., Hu, B., Zhou, Y., et al. (2019). miRNA-21 Promotes Osteogenesis via the PTEN/PI3K/Akt/HIF-1α Pathway and Enhances Bone Regeneration in Critical Size Defects. *Stem Cell Res. Ther.* 10 (1), 65. doi:10.1186/s13287-019-1168-2

Yang, K., Zhang, S., He, J., and Nie, Z. (2021). Polymers and Inorganic Nanoparticles: A Winning Combination towards Assembled Nanostructures for Cancer Imaging and Therapy. *Nano Today* 36, 101046. doi:10.1016/j.nantod.2020.101046

Yang, L., He, X., Jing, G., Wang, H., Niu, J., Qian, Y., et al. (2021). Layered Double Hydroxide Nanoparticles with Osteogenic Effects as miRNA Carriers to Synergistically Promote Osteogenesis of MSCs. *ACS Appl. Mat. Interfaces* 13 (41), 48386–48402. doi:10.1021/acsami.1c14382

Yoshizuka, M., Nakasa, T., Kawanishi, Y., Hachisuka, S., Furuta, T., Miyaki, S., et al. (2016). Inhibition of microRNA-222 Expression Accelerates Bone Healing with Enhancement of Osteogenesis, Chondrogenesis, and Angiogenesis in a Rat Refractory Fracture Model. *J. Orthop. Sci.* 21 (6), 852–858. doi:10.1016/j.jos.2016.07.021

Yu, M., Xue, Y., Ma, P. X., Mao, C., and Lei, B. (2017). Intrinsic Ultrahigh Drug/miRNA Loading Capacity of Biodegradable Bioactive Glass Nanoparticles

toward Highly Efficient Pharmaceutical Delivery. *ACS Appl. Mat. Interfaces* 9 (10), 8460–8470. doi:10.1021/acsami.6b13874

Yuan, X., Han, L., Lin, H., Guo, Z., Huang, Y., Li, S., et al. (2019). The Role of antimiR-26a-5p/biphasic Calcium Phosphate in Repairing Rat Femoral Defects. *Int. J. Mol. Med.* 44 (3), 857–870. doi:10.3892/ijmm.2019.4249

Zare, H., Ahmadi, S., Ghasemi, A., Ghanbari, M., Rabiee, N., Bagherzadeh, M., et al. (2021). Carbon Nanotubes: Smart Drug/Gene Delivery Carriers. *Int. J. Nanomedicine* 16, 1681–1706. doi:10.2147/ijn.S299448

Zhang, X., Li, Y., Chen, Y. E., Chen, J., and Ma, P. X. (2016). Cell-free 3D Scaffold with Two-Stage Delivery of miRNA-26a to Regenerate Critical-Sized Bone Defects. *Nat. Commun.* 7, 10376. doi:10.1038/ncomms10376

Zhang, Q., Lin, S., Shi, S., Zhang, T., Ma, Q., Tian, T., et al. (2018). Anti-inflammatory and Antioxidative Effects of Tetrahedral DNA Nanostructures via the Modulation of Macrophage Responses. *ACS Appl. Mat. Interfaces* 10 (4), 3421–3430. doi:10.1021/acsami.7b17928

Zhang, L., Yang, G., Johnson, B. N., and Jia, X. (2019). Three-dimensional (3D) Printed Scaffold and Material Selection for Bone Repair. *Acta Biomater.* 84, 16–33. doi:10.1016/j.actbio.2018.11.039

Zhang, J., Zhang, T., Tang, B., Li, J., and Zha, Z. (2021). The miR-187 Induced Bone Reconstruction and Healing in a Mouse Model of Osteoporosis, and Accelerated Osteoblastic Differentiation of Human Multipotent Stromal Cells by Targeting BARX2. *Pathology - Res. Pract.* 219, 153340. doi:10.1016/j.prp.2021.153340

Zhang, Y., Zhuang, Z., Wei, Q., Li, P., Li, J., Fan, Y., et al. (2021). Inhibition of miR-93-5p Promotes Osteogenic Differentiation in a Rabbit Model of Trauma-induced Osteonecrosis of the Femoral Head. *FEBS Open Bio* 11, 2152–2165. doi:10.1002/2211-5463.13218

Zhang, Z., Jiang, W., Hu, M., Gao, R., and Zhou, X. (2021). MiR-486-3p Promotes Osteogenic Differentiation of BMSC by Targeting CTNNBIP1 and Activating the Wnt/β-Catenin Pathway. *Biochem. Biophysical Res. Commun.* 566, 59–66. doi:10.1016/j.bbrc.2021.05.098

Zhao, C., Sun, W., Zhang, P., Ling, S., Li, Y., Zhao, D., et al. (2015). miR-214 Promotes Osteoclastogenesis by Targeting Pten/PI3k/Akt Pathway. *RNA Biol.* 12 (3), 343–353. doi:10.1080/15476286.2015.1017205

Zhao, C., Gu, Y., Wang, Y., Qin, Q., Wang, T., Huang, M., et al. (2021). miR-129-5p Promotes Osteogenic Differentiation of BMSCs and Bone Regeneration via Repressing Dkk3. *Stem Cells Int.* 2021, 18. doi:10.1155/2021/7435605

Zhou, Y., Chen, X., Zhu, Z., Bi, D., and Ma, S. (2021). MiR-133a Delivery to Osteoblasts Ameliorates Mechanical Unloading-Triggered Osteopenia Progression *In Vitro* and *In Vivo*. *Int. Immunopharmacol.* 97, 107613. doi:10.1016/j.intimp.2021.107613